



## 4-Chlorophenylthioacetone-derived thiosemicarbazones as potent antitrypanosomal drug candidates: Investigations on the mode of action

Diego Rodney Rodrigues de Assis<sup>a</sup>, Alexandre Almeida Oliveira<sup>b</sup>, Samuel Luiz Porto<sup>a</sup>, Rayane Aparecida Nonato Rabelo<sup>a</sup>, Eduardo Burgarelli Lages<sup>c</sup>, Viviane Corrêa Santos<sup>a</sup>, Matheus Marques Milagre<sup>d</sup>, Stenio Perdigão Fragoso<sup>e</sup>, Mauro Martins Teixeira<sup>a</sup>, Rafaela Salgado Ferreira<sup>a</sup>, Carlos Renato Machado<sup>a</sup>, Lucas Antônio Miranda Ferreira<sup>c</sup>, Nivaldo Lucio Speziali<sup>f</sup>, Heloisa Beraldo<sup>b,\*</sup>,<sup>1</sup>, Fabiana Simão Machado<sup>a,g,\*</sup>,<sup>1</sup>

<sup>a</sup> Departamento de Bioquímica e Imunologia, Instituto de Ciências Biológicas, Universidade Federal de Minas Gerais, 31270-901 Belo Horizonte, MG, Brazil

<sup>b</sup> Departamento de Química, Instituto de Ciências Exatas, Universidade Federal de Minas Gerais, 31270-901 Belo Horizonte, MG, Brazil

<sup>c</sup> Departamento de Produtos Farmacêuticos, Faculdade de Farmácia, Universidade Federal de Minas Gerais 31270-901 Belo Horizonte, MG, Brazil

<sup>d</sup> Escola de Farmácia, Universidade Federal de Ouro Preto, 35400-000 Ouro Preto, MG, Brazil

<sup>e</sup> Fundação Oswaldo Cruz, Instituto Carlos Chagas, 81350-010 Curitiba, PR, Brazil

<sup>f</sup> Departamento de Física, Instituto de Ciências Exatas, Universidade Federal de Minas Gerais, 31270-901 Belo Horizonte, MG, Brazil

<sup>g</sup> Faculdade de Medicina, Programa em Ciências da Saúde: Infectologia e Medicina Tropical, Universidade Federal de Minas Gerais, Belo Horizonte, MG, Brazil

### ARTICLE INFO

#### Keywords:

*Trypanosoma cruzi*  
Chagas disease  
Hydrazones  
Thiosemicarbazones  
Treatment  
Lipid nanoparticles

### ABSTRACT

Chagas disease (ChD), caused by *Trypanosoma cruzi*, remains a challenge for the medical and scientific fields due to the inefficiency of the therapeutic approaches available for its treatment. Thiosemicarbazones and hydrazones present a wide spectrum of bioactivities and are considered a platform for the design of new anti-*T. cruzi* drug candidates. Herein, the potential antichagasic activities of [(*E*)-2-(1-(4-chlorophenylthio)propan-2-ylidene)hydrazinecarbothioamides] (**C1**, **C3**), [(*E*)-*N*'-(1-((4-chlorophenyl)thio)propan-2-ylidene)benzohydrazide] (**C2**), [(*E*)-2-(1-(4-, and [(*E*)-2-(1-((4-chlorophenyl)thio)propan-2-ylidene)hydrazinecarboxamide] (**C4**) were investigated. Macrophages (MOs) from C57BL/6 mice stimulated with **C1** and **C3**, but not with **C2** and **C4**, reduced amastigote replication and trypomastigote release, independent of nitric oxide (NO) and reactive oxygen species production and indoleamine 2,3-dioxygenase activity. **C3**, but not **C1**, reduced parasite uptake by MOs and potentiated TNF production. In cardiomyocytes, **C3** reduced trypomastigote release independently of NO, TNF, and IL-6 production. **C1** and **C3** were non-toxic to the host cells. A reduction of parasite release was found during infection of MOs with trypomastigotes pre-incubated with **C1** or **C3** and MOs pre-stimulated with compounds before infection. Moreover, **C1** and **C3** acted directly on trypomastigotes, killing them faster than Benznidazole, and inhibited *T. cruzi* proliferation at various stages of its intracellular cycle. Mechanistically, **C1** and **C3** inhibit parasite duplication, and this process cannot be reversed by inhibiting the DNA damage response. *In vivo*, **C1** and **C3** attenuated parasitemia in *T. cruzi*-infected mice. Moreover, **C3** loaded in a lipid nanocarrier system (nanoemulsion) maintained anti-*T. cruzi* activity *in vivo*. Collectively, these data suggest that **C1** and **C3** are candidates for the treatment of ChD and present activity in both the host and parasite cells.

**Abbreviations:** MTT, 3-(4,5-Dimethyl-2-thiazolyl)-2,5-diphenyl-2H-tetrazolium bromide; Bz, benzimidazole; CMs, cardiomyocytes; ChD, Chagas disease; DMSO, Dimethyl Sulfoxide; IDO, indoleamine 2,3-dioxygenase; iNOS, inducible nitric oxide synthase; IFN- $\gamma$ , interferon gamma; IL, interleukin; LDH, lactate dehydrogenase; MOs, macrophages; NE, nanoemulsion; Nfx, nifurtimox; NO, nitric oxide; ROS, reactive oxygen species; TNF, tumor necrosis factor.

\* Corresponding authors at: Departamento de Bioquímica e Imunologia, Instituto de Ciências Biológicas (F. Machado) and Departamento de Química, Instituto de Ciências Exatas (H. Beraldo), Universidade Federal de Minas Gerais, 31270-901 Belo Horizonte, MG, Brazil

E-mail address: [machadofs@icb.ufmg.br](mailto:machadofs@icb.ufmg.br) (F. Simão Machado).

<sup>1</sup> These authors contributed equally to this manuscript.

<https://doi.org/10.1016/j.bioorg.2021.105018>

Received 16 March 2021; Received in revised form 19 May 2021; Accepted 20 May 2021

Available online 25 May 2021

0045-2068/© 2021 Elsevier Inc. All rights reserved.

## 1. Introduction

More than 100 years after its discovery, ChD, which is caused by *Trypanosoma cruzi*, remains a serious problem due to its high morbidity. It is estimated that eight million people are infected with *T. cruzi* worldwide, mainly in Latin America, where this disease remains a public health problem, causing disability in infected individuals and more than 10,000 deaths per year [1]. ChD is characterized mainly by two distinct phases: acute and chronic. The chronic phase is considered to be of greater relevance, in which approximately 30% of patients present with pathogenesis, including chronic cardiomyopathy (myocarditis, heart failure, and eventually sudden death) and digestive alterations (megaesophagus and megacolon) [2].

During parasite-host interaction, cells of the mononuclear phagocytic system, mainly macrophages (MOs), play a fundamental role in decreasing parasitemia by controlling *T. cruzi* proliferation. These cells respond to pathogen-associated molecular patterns (e.g., lipids, carbohydrates, nucleic acids, and various proteins derived from the parasite) and orchestrate a Th1-type response (activation of natural killer cells and TCD4<sup>+</sup> lymphocytes), primarily through the production of IFN- $\gamma$ , IL-12, and TNF cytokines [3]. These cytokines are crucial for activating oxygen-dependent mechanisms such as production of reactive oxygen species (ROS), and oxygen-independent (such as nitric oxide – NO production) [4,5] trypanocidal mechanisms. In addition, other trypanocidal mechanisms that involve nutrient deprivation (such as indoleamine 2,3-dioxygenase enzyme – IDO – activation) are also important for limiting the intracellular growth of *T. cruzi*, because IDO activity reduces the levels of tryptophan, an amino acid involved in *T. cruzi* multiplication. Moreover, IDO activation results in release of sub-products that are toxic to the parasite [6]. Cardiomyocytes are also involved in the development of ChD pathogenesis because these cells actively participate in the control of parasite replication by producing and responding to inflammatory molecules [7].

Benznidazole (Bz) and nifurtimox (Nfx) are the only drugs considered effective for the treatment of the acute phase of human Chagas infection. However, these therapeutics present very low cure rates in the chronic phase of the disease. Furthermore, when used for long-term regimens (30 to 60 days), both drugs cause undesirable side effects in 30% to 87% of patients, resulting in treatment interruptions [8,9]. Thus, the search for new antichagasic drug candidates with high efficacy and minimal toxicity is extremely relevant.

Thiosemicarbazones and hydrazones are Schiff base compounds, which exhibit a wide range of pharmacological applications as anti-neoplastic, antimicrobial, and antiparasitic agents. The anti-trypanosomal activities of thiosemicarbazones, hydrazones, and their

metal complexes have been extensively reported [10-12]. Thiophenol-2-ylidene-thiosemicarbazones and thiazolylhydrazones, which have a spacer group (-S-CH<sub>2</sub>) between the phenyl ring and the hydrazone/thiosemicarbazone backbone (see Fig. 1), have shown promising anti-*T. cruzi* activities [13,14].

Currently, targets including cruzain protease [15], DNA damage response (DDR) [16], and topoisomerase enzymes from *T. cruzi* [17] have been investigated in drug development due to their capacity to interfere with pathways that are crucial for *T. cruzi* survival. Thiazolylhydrazones have been shown to act as inhibitors of cruzain [18].

In the present work, a family of 4-chlorophenylthioacetone-derived hydrazones and thiosemicarbazones (Fig. 1) were obtained, and their anti-trypanosomal activities were evaluated. Our investigation aimed to elucidate their mechanism of action and their molecular targets, in both host and parasite cells.

The critical steps in developing an effective drug include effective absorption by the host, protection against chemical and/or enzymatic degradation, and half-life improvement. Several research groups have resorted to the use of drug delivery systems based on lipid nanocarriers [19], mainly for compounds with reduced pharmacological activity due to low solubility in aqueous media, such as certain hydrophobic hydrazones and thiosemicarbazones [19]. Hence, lipid nanocarrier formulations of the compounds were also prepared, and their antiparasitic activities were tested. Thus, the compounds under study and their nanocarrier formulations were investigated as a platform for the development of new drug candidates for the treatment of ChD.

## 2. Materials and methods

### 2.1. Ethics statement

This research study was carried out in strict accordance with the Brazilian guidelines on animal work and the Guide for the Care and Use of Laboratory Animals of the National Institute of Health (NIH). The animal ethics committee (CEUA) of *Universidade Federal de Minas Gerais* (UFMG) – Brazil (BR), approved all experiments and procedures (Permit Number 414/2018).

### 2.2. Synthesis and characterization of C1-C4.

The reagents were purchased from Aldrich and used as received. Partial elemental analyses were performed on a Perkin Elmer CHN 2400 analyzer. Melting points were determined with a Mettler MQAPF-302 apparatus. Infrared spectra were recorded on a Perkin Elmer Spectrum One equipment employing the attenuated total reflectance (ATR)

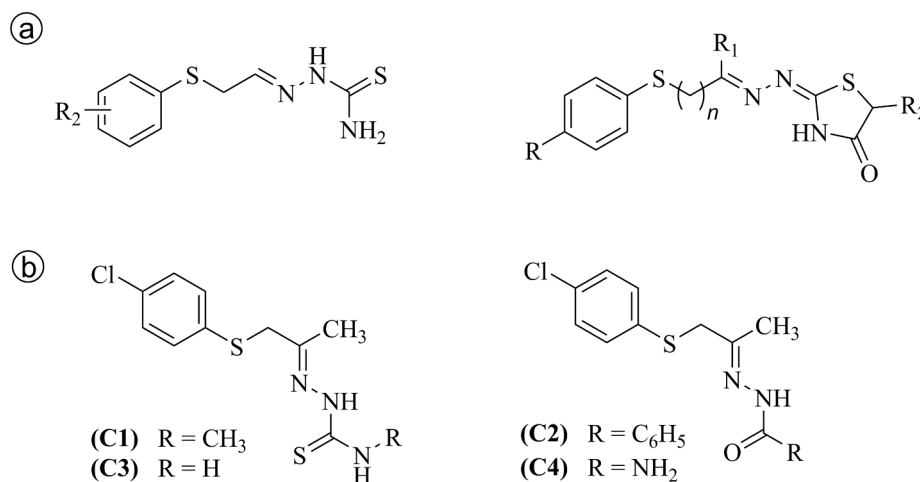


Fig. 1. (a) Compounds studied by other authors [13,14]; (b) 4-chlorophenylthioacetone-derived thiosemicarbazones (C1, C3) and hydrazones (C2, C4) studied in the present work.

method (4000–400  $\text{cm}^{-1}$ ). NMR spectra were obtained at 25 °C with a Bruker DPX-400 Advance (400 MHz) spectrometer using  $\text{DMSO-}d_6$  as solvent. Mass spectra were recorded with a Shimadzu LCMS-IT-TOF instrument working at high-resolution.

Single crystal X-ray diffraction measurements were carried out on an Oxford-Diffraction GEMINI-Ultra diffractometer (LabCri-UFMG) using graphite-Enhance Source Mo  $K\alpha$  radiation ( $\lambda = 0.71073 \text{ \AA}$ ) at 293(2) K. Data collection, cell refinements and data reduction were performed using the CrysAlisPro software package [20]. An absorption correction based on a multi-scan method was applied. The structures were solved by direct methods using SHELXS-2013/1 [21]. Full-matrix least-squares refinement procedure on  $F^2$  with anisotropic thermal parameters was carried out using SHELXL-2014/7 [22]. Positional and anisotropic atomic displacement parameters were refined for all non-hydrogen atoms. Hydrogen atoms were placed geometrically and the positional parameters were refined using a riding model. Suitable single crystals of **C1** and **C3** were obtained at room temperature from slow evaporation of a 9:1 methanol: DMSO solution of the compounds. A summary of the crystal data, data collection details and refinement results is listed in **Table S1 (Supplementary Material)**. Molecular graphics were plotted using PLATON [23].

### 2.3. Syntheses of the 4-chlorophenylthioacetone-derived thiosemicarbazones and hydrazones

The thiosemicarbazones and hydrazones were prepared as previously described [24]. Briefly, in a 50 mL flask containing 10 mL of methanol, 207 mg (1 mmol) of (4-chlorophenylthio) acetone were solubilized. Three drops of acetic acid were added and, after 10 min with stirring, 1 mmol of the appropriate thiosemicarbazide or hydrazide was added. In all cases, the reaction mixture was kept under magnetic stirring and reflux for 4 h (see **Scheme 1**). After cooling at room temperature, the mixture was kept in the freezer for 24 h, then it was filtered, washed with a minimum of methanol and diethyl ether, and the solids were subsequently dried in a desiccator under reduced pressure.

The compounds were characterized by elemental analysis and by means of their infrared, NMR and HRMS spectra. The carbon atom numbering scheme and all spectra of **C1** - **C4** are shown in the Supplementary Material.

#### 2.3.1. [(E)-2-(1-(4-chlorophenylthio)propan-2-ylidene)-N-methylhydrazinecarbothioamide] (**C1**)

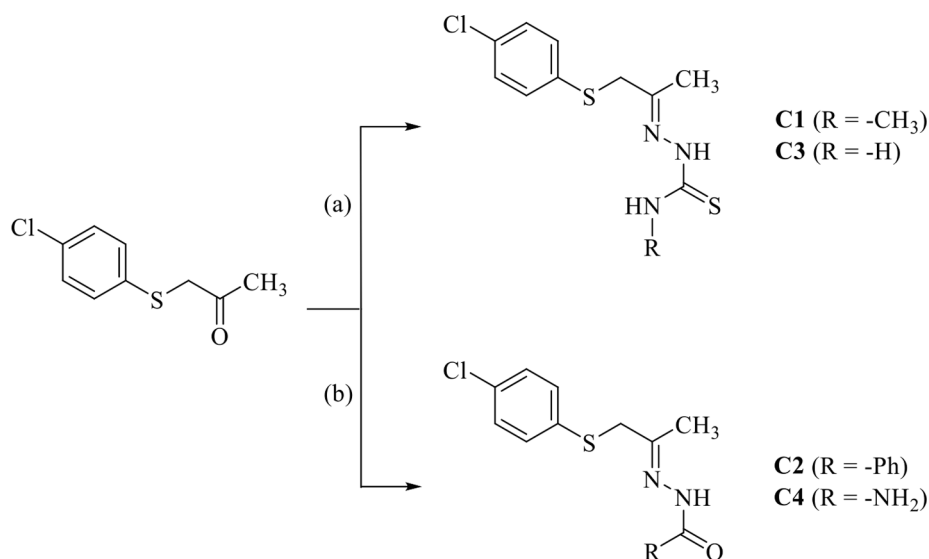
White-yellowish solid. Yield: 64%. Melting point: 106.4 °C – 108.1 °C. Anal. Calc. for  $\text{C}_{11}\text{H}_{14}\text{ClN}_3\text{S}_2$ : C, 45.90; H, 4.90; N, 14.60. Found: C, 45.94; H, 4.88; N, 14.44. FW: 287.82  $\text{g mol}^{-1}$ . IR (ATR,  $\text{cm}^{-1}$ ): 3188  $\nu(\text{N2-H})$ , 1520  $\nu(\text{C} = \text{N1})$ , 848  $\nu(\text{C}=\text{S})$ .  $^1\text{H NMR}$  [400.13 MHz,  $\text{DMSO-}d_6$ ,  $\delta$  (ppm)]: 10.12 [s, 1H, N2H], 8.10 [d, 1H, N3H], 7.42 [d, 2H, H3, H5], 7.33 [d, 2H, H2, H6], 3.82 [s, 2H, H7], 2.96 [d, 3H, H11], 1.96 [s, 3H, H9].  $^{13}\text{C NMR}$  [100.61 MHz,  $\text{DMSO-}d_6$ ,  $\delta$  (ppm)]: 178.6 [C10], 148.0 [C8], 134.1 [C4], 130.8 [C1], 130.6 [C3, C5], 128.8 [C2, C6], 40.1 [C7], 30.8 [C11], 15.1 [C9]. HRMS [ESI(+), IT-TOF] calculated for  $\text{C}_{11}\text{H}_{15}\text{ClN}_3\text{S}_2$ ,  $[\text{M} + \text{H}]^+$ : 288.0396, found 288.0389.

#### 2.3.2. [(E)-N'-(1-((4-chlorophenyl)thio)propan-2-ylidene)benzohydrazide] (**C2**)

White solid. Yield: 57%. Melting point: 126.7 °C – 128.2 °C. Anal. Calc. for  $\text{C}_{16}\text{H}_{15}\text{ClN}_2\text{OS}$ : C, 60.28; H, 4.74; N, 8.79. Found: C, 60.13; H, 4.58; N, 8.87. FW: 318.82  $\text{g mol}^{-1}$ . IR (ATR,  $\text{cm}^{-1}$ ): 3243  $\nu(\text{N2-H})$ , 1520  $\nu(\text{C} = \text{N1})$ , 1650  $\nu(\text{C}=\text{O})$ .  $^1\text{H NMR}$  [400.13 MHz,  $\text{DMSO-}d_6$ ,  $\delta$  (ppm)]: 10.55 [s, 1H, N2H], 7.82 [s, 2H, H12, H16], 7.60–7.50 [m, 1H, H14], 7.50–7.40 [m, 4H, H3, H5, H13, H15], 7.35 [d, 2H, H2, H6], 3.90 [s, 2H, H7], 2.05 [s, 3H, H9].  $^{13}\text{C NMR}$  [100.61 MHz,  $\text{DMSO-}d_6$ ,  $\delta$  (ppm)]: 163.5 [C10], 157.1 [C8], 134.6 [C4], 133.9 [C11], 131.4 [C14], 130.8 [C1], 130.4 [C3, C5], 128.8 [C2, C6], 128.2 [C13, C15], 127.8 [C12, C16], 40.6 [C7], 15.7 [C9]. HRMS [ESI(+), IT-TOF] calculated for  $\text{C}_{16}\text{H}_{16}\text{ClN}_2\text{OS}$ ,  $[\text{M} + \text{H}]^+$ : 319.0672, found 319.0690.

#### 2.3.3. [(E)-2-(1-(4-chlorophenylthio)propan-2-ylidene)hydrazinecarbothioamide] (**C3**)

White solid. Yield: 83%. Melting point: 136.3 °C – 137.0 °C. Anal. Calc. for  $\text{C}_{10}\text{H}_{12}\text{ClN}_3\text{S}_2$ : C, 43.87; H, 4.42; N, 15.35. Found: C, 43.85; H, 4.40; N, 15.14. FW: 273.80  $\text{g mol}^{-1}$ . IR (ATR,  $\text{cm}^{-1}$ ): 3150  $\nu(\text{N2-H})$ , 1591  $\nu(\text{C} = \text{N1})$ , 864  $\nu(\text{C}=\text{S})$ .  $^1\text{H NMR}$  [400.13 MHz,  $\text{DMSO-}d_6$ ,  $\delta$  (ppm)]: 10.10 [s, 1H, N2H], 8.13 [s, 1H, N3H], 7.54 [s, 1H, N3H], 7.41 [d, 2H, H3, H5], 7.32 [d, 2H, H2, H6], 3.82 [s, 2H, H7], 1.96 [s, 3H, H9].  $^{13}\text{C NMR}$  [100.61 MHz,  $\text{DMSO-}d_6$ ,  $\delta$  (ppm)]: 178.8 [C10], 148.2 [C8], 134.0 [C4], 130.7 [C1], 130.3 [C3, C5], 128.7 [C2, C6], 39.8 [C7], 15.1 [C9]. HRMS [ESI(+), IT-TOF] calculated for  $\text{C}_{10}\text{H}_{12}\text{ClN}_3\text{NaS}_2$ ,  $[\text{M} + \text{Na}]^+$ : 296.0059, found 296.0065.



**Scheme 1.** Syntheses of (4-chlorophenylthio)acetone-derived thiosemicarbazones (**C1**, **C3**) and hydrazones (**C2**, **C4**). Reagents and conditions: (a) thiosemicarbazide, MeOH, acetic acid (three drops), reflux, 4 h; (b) hydrazide, MeOH, acetic acid (three drops), reflux, 4 h.

### 2.3.4. [(E)-2-(1-((4-chlorophenyl)thio)propan-2-ylidene)hydrazinecarboxamide] (C4)

White-yellowish solid. Yield: 75%. Melting point: 158.2 °C – 161.1 °C. Anal. Calc. for C<sub>10</sub>H<sub>12</sub>ClN<sub>3</sub>O<sub>2</sub>: C, 46.60; H, 4.69; N, 16.30. Found: C, 46.09; H, 4.53; N, 16.24. FW: 257.74 g mol<sup>-1</sup>. IR (ATR, cm<sup>-1</sup>): 3164 ν(N2-H), 1584 ν(C = N1), 1685 ν(C=O). <sup>1</sup>H NMR [400.13 MHz, DMSO-d<sub>6</sub>, δ (ppm)]: 9.12 [s, 1H, N2H], 7.40 [d, 2H, H3, H5], 7.32 [d, 2H, H2, H6], 6.24 [s, 2H, N3H], 3.78 [s, 2H, H7], 1.85 [s, 3H, H9]. <sup>13</sup>C NMR [100.61 MHz, DMSO-d<sub>6</sub>, δ (ppm)]: 157.1 [C10], 143.8 [C8], 134.4 [C4], 130.5 [C1], 130.3 [C3, C5], 128.7 [C2, C6], 40.1 [C7], 14.5 [C9]. HRMS [ESI(+), IT-TOF] calculated for C<sub>10</sub>H<sub>13</sub>ClN<sub>3</sub>O<sub>2</sub>, [M + H]<sup>+</sup>: 258.0468, found 258.0478.

## 2.4. Preparation of a C3 lipid nanocarrier

C3 was encapsulated in a lipid nanocarrier (nanoemulsion - NE), according to the composition described in the Table 1. The oily and aqueous phases were weighed separately and heated to 80 °C. After fusion of the lipids, the aqueous phase was slowly poured over the oil phase under constant agitation at 800 rpm using the Ultra Turrax T-25 homogenizer (Ika Labortechnik, Germany). After 2 min, the emulsion was sonicated (21% amplitude, 10 min) using a high-intensity ultrasonic processor (model CPX 500, Cole-Palmer Instruments, USA). The obtained emulsion was cooled to room temperature under magnetic stirring. The pH was adjusted to 7.0 and the final volume was completed to 10 mL with water. The formulation was stored at 4 °C, protected from light and in a nitrogen atmosphere.

### 2.4.1. Nanoemulsion characterization

The nanoemulsion (NE) formulation was characterized by its average particle diameter, polydispersity index (PI), zeta potential (Zp), and encapsulation efficiency (EE). The average particle diameter and PI were measured by means of dynamic light scattering (DLS) using a Zetasizer Nano ZS90 (Malvern Instruments, United Kingdom) at a fixed angle of 90° and temperature of 25 °C. Measurements of Zp were performed by dynamic light scattering (DLS) determinations of electrophoretic mobility at 25 °C. To carry out the analyses, 10 µL of the formulation was diluted in 1 mL of distilled water.

To determine the EE of the compound, filtration and ultrafiltration methods were used. Thus, the procedure was divided into three stages: total, filtered, and ultrafiltered. In the first (total concentration) stage, 500 µL of the formulation was transferred to a 5 mL volumetric flask. Tetrahydrofuran (THF, 2 mL) was added. Then, 300 µL were transferred to a 5 mL volumetric flask, and the volume was completed with DMSO. In the second step (filtration), 1 mL of the formulation was filtered through a 0.45 µm membrane. Then, 500 µL of the filtrate were transferred to a 5 mL volumetric flask, 2 mL of THF were added, and the volume was completed with DMSO. Then, 300 µL were transferred to a 5 mL volumetric flask, and the volume was again completed with DMSO. In the third stage (ultrafiltration), 300 µL of the formulation were transferred to an Amicon 100 kDa filtration device (Millipore, USA), which was subjected to centrifugation at 2400 × g for 10 min. Then, 50 µL of the filtrate were transferred to an eppendorf, and 450 µL of DMSO were added. The concentration of C3 in all analyses was evaluated by UV-VIS spectrometry, using the absorbance at 280 nm. EE was

**Table 1**  
Composition of the nanoemulsion (NE) containing C3.

Formulation (NE)			
Oily phase		Aqueous phase	
MCT	5.0%	Glycerol	2.25%
Cholesterol	0.5%	Water qsp	100%
Tween 80	1.5%		
C3	0.1%		
MCT: medium-chain triglycerides			

calculated using the following formula:

$$EE(\%) = \frac{[\text{Total}] - [\text{Filtered}] - \text{Ultrafiltrate}}{[\text{Total}]} \times 100$$

*Ultrafiltrate*: represents the fraction of the compound soluble in the aqueous phase of the formulation. *Filtered*: represents the fraction of the compound insoluble in the aqueous phase of the formulation; *Total*: the sum of the drug fraction retained in the lipid matrix (encapsulated), the fraction soluble in the aqueous phase, and the insoluble fraction in the aqueous phase.

## 2.5. Animals

Wild-type (WT) C57BL/6 mice, female, aged 8–10 weeks, were obtained from the Animal Care Facilities of *Universidade Federal de Minas Gerais*. Inducible nitric oxide synthase knockout (iNOS KO), gp91<sup>Phox</sup> knockout (Phox KO), and indoleamine 2,3 dioxygenase knockout (IDO KO) female mice were bred on a C57BL/6 genetic background under pathogen-free conditions at the *Instituto de Ciências Biológicas, Universidade Federal de Minas Gerais*, Brazil.

### 2.6. Infection of mice and cells

The *T. cruzi* Y strain was used for both *in vivo* and *in vitro* experiments. C57BL/6 mice were infected intraperitoneally (i.p.) with 1x10<sup>3</sup> trypomastigotes, and parasitemia levels were periodically measured in 5 µL of blood from the tail vein. For *in vitro* infection, trypomastigotes were grown in cultures of a monkey kidney epithelial cell line (LLC-MK2) and then used for infection at a 5:1 parasite/host cell ratio [7].

### 2.7. Macrophage cultures, treatment, and NO-inhibition

MOs were harvested from peritoneal cavities as previously described [7], from C57BL/6 (WT), iNOS KO, Phox KO, or IDO KO mice, and plated (2x10<sup>5</sup> or 1x10<sup>6</sup> cell/well – 96 or 24 well, respectively) onto culture plates (Nunc, Rochester, NY, USA). Infections were performed as described above. Cells were treated with C1 - C4 at concentrations in the 10 µM – 50 µM range. IFN-γ at 100 ng/mL (Sigma) was used as a positive control for *T. cruzi* replication in MOs. In addition, WT and Phox KO MOs were infected with *T. cruzi* (as described above) and posteriorly stimulated with C1 (20 µM), C3 (30 µM), or IFN-γ (100 ng/mL). Simultaneously, the arginine amino acid analog N<sup>G</sup>-monomethyl-L-arginine (L-NMMA) (Sigma-Aldrich Co.) was added at 400 µM, to inhibit NO production [7]. MOs were treated with compounds at 2, 6, 12, and 24 h after infection to evaluate the impact of the compounds on amastigote replication and differentiation.

### 2.8. Cardiomyocyte H9c2-line culture, infection, and treatment

Adherent H9c2 rat embryonic cardiomyocytes (CMs), H9c2(2–1) (ATCC® CRL-1446™) were grown in Dulbecco's Modified Eagle Medium (DMEM – Cultilab, Campinas, SP/BR), pH 7.6, supplemented with 10% fetal bovine serum (Cultilab) and 1% penicillin/streptomycin (Gibco, BLR Life Technologies). Cells were cultured at 37 °C in 5% CO<sub>2</sub>. Before reaching confluence, the cells were removed from the bottle using trypsin/EDTA (Sigma) and centrifuged for 10 min at 500×g. The pellet was homogenized in DMEM, and cells were counted in a Neubauer's chamber with the aid of trypan blue stain (Gibco) and seeded at a density of 4x10<sup>4</sup> cells/well. These cells were infected as described above, and after 2 h of infection, C3 or IFN-γ was added at 0.62 µM – 5 µM or 100 ng/ml, respectively.

### 2.9. Parasite count

The number of intracellular amastigotes was determined in macrophages fixed and stained with *Panótico Rápido* (LB Laborclin, Pinhais,

PR/BR) at four and 24/48 h post-infection, to evaluate parasite uptake and intracellular growth, respectively. The number of released trypomastigotes from MOs and CMs was quantified in the supernatants from three to seven days post-infection (dpi), as previously described [25].

#### 2.10. Nitric oxide and cytokines determinations

Nitric oxide determination was performed in supernatants by the Griess colorimetric method as previously described [26]. Optical densities were measured at 540 nm in a plate reader (96 wells) (Elx800 - Bio Tek). TNF and IL-6 cytokines were assayed in the supernatants of the macrophage cultures by the sandwich enzyme-linked immunosorbent assay (ELISA) method, according to the manufacturer's instructions (R & D Systems Inc., Minneapolis, Minnesota). Optical densities were measured at 450 nm in a plate reader (96 wells) (Elx800 - Bio Tek).

#### 2.11. LDH assay

At 24 or 48 h after treatment with **C1** and **C3**, the culture supernatants (from MOs and CMs) were collected for cytotoxicity assay (LDH - lactate dehydrogenase). The LDH test is a marker of plasma membrane integrity [27]. The assay consists of removing the supernatant from cells and measuring the activity of the released enzyme by offering its substrate (Bioclin® Kit, Belo Horizonte, MG/BR).

#### 2.12. Pre-incubation of macrophages and *T. cruzi*-trypomastigotes with **C1** or **C3**

MOs were plated as above; however, before infection with the parasite, the cells were stimulated with **C1**, **C3**, or IFN- $\gamma$  for 1 h. After this interval, the cells were washed twice with RPMI and then infected (as above). Trypomastigotes were obtained as described above, counted, and incubated with RPMI in the presence of **C1** (30  $\mu$ M) or **C3** (20  $\mu$ M). Incubation occurred in microtubes for 1 h (37 °C, 5% CO<sub>2</sub>). After incubations, the "mix" parasite "**C1** + *T. cruzi*" or "**C3** + *T. cruzi*" was centrifuged at 2438  $\times$  g for 10 min. The parasites were resuspended in RPMI medium for subsequent MO infection (as described above).

#### 2.13. Trypomastigotes incubation with **C1**, **C3** and benzimidazole

Trypomastigotes (Y strain) from LLC-MK2 cells were cultured in the presence of RPMI alone, **C1** (30  $\mu$ M), **C3** (20  $\mu$ M), or Benzimidazole (30  $\mu$ M) for 1 h. After incubation, the parasites were centrifuged (2438  $\times$  g, 10 min) to remove the compounds and resuspended in RPMI culture medium. A second experimental group remained in the presence of the compounds throughout the analysis. Viable parasites (flagellar movement and elongated morphology characteristic of trypomastigote forms) were observed under an optical microscope and counted in a Neubauer's chamber at two, four, and six h after initial treatment.

#### 2.14. Epimastigotes culture, treatment, and caffeine-pretreatment

Epimastigotes (Y strain - WT, DM28 strain - WT, topoisomerase 3 $\alpha$  KO DM28 strain) were grown in liver infusion tryptose (LIT) medium (pH 7.4) supplemented with 10% fetal bovine serum (FBS, Gibco BRL, Invitrogen, Carlsbad, CA, USA) and 1% streptomycin/penicillin (Gibco) at 28 °C. Parasite transfection (Topo-3 $\alpha$  KO background DM28) was performed using electroporation, as previously described [28]. Cells were cultured until the logarithmic growth phase before all experiments. For the pretreatment assay, epimastigotes were incubated, or not, with caffeine (Sigma) at doses of 1 mM to 4 mM for 1 h. After caffeine incubation, parasites were centrifuged (2438  $\times$  g, 10 min), seeded in culture plates, and stimulated, or not, with 30  $\mu$ M of **C1**, **C3**, or Bz. The parasite growth profile was followed from three to 48 h after treatment.

#### 2.15. MTT assay

Parasites were seeded (1 $\times$ 10<sup>6</sup>/well) in 96-well plates in the presence or absence of compound. After treatment, 10  $\mu$ L of MTT (Sigma) solution (5 mg/mL) was added to the wells, and immediately afterwards, the plates were incubated at 37 °C for 2 h, for the trypomastigotes assay, or 28 °C for 2 h, for the epimastigotes assay. After this period, the parasites were removed from the plates, placed in 1.5 mL tubes, and centrifuged (2438  $\times$  g, 10 min). The supernatants were discarded, and the pellet was resuspended in 200  $\mu$ L of DMSO to dissolve formazan crystals. A 200  $\mu$ L aliquot was pipetted into a 96-well plate for reading on a spectrophotometer at a wavelength of 490 nm. The results were expressed as optical density (OD) and compared with the OD values obtained from the control group.

#### 2.16. Cruzain inhibition assay

The catalytic activity of cruzain was monitored by the cleavage of the fluorogenic substrate Z-Phe-Arg-amidomethylcoumarin (Z-FR-AMC) in a Synergy 2 plate reader (Biotek), as previously described [29]. For this purpose, 4 nM cruzain was incubated in the presence of **C1**, **C3**, or Bz at 100  $\mu$ M for 10 min at room temperature. Then, 2.5  $\mu$ M of the substrate was added to start the reaction. The positive control for inhibition (E64) was used. The assays were performed in triplicate using 0.1 M sodium acetate (pH 5.5) in the presence of 5 mM beta-mercaptoethanol and 0.01% Triton X-100 in a 96-well plate (flat black background). Aggregation assays were performed as previously described [30], with the following modification: the inhibitory activity of the compounds was evaluated in the presence of 0.001%, 0.01%, and 0.1% Triton X-100. For IC<sub>50</sub> determination, the activity of **C3** was evaluated in eleven concentrations, ranging from 0.0015  $\mu$ M to 500  $\mu$ M. Two independent experiments were performed in triplicate, and the data were analyzed with GraphPad Prism 5.0, employing a nonlinear regression analysis of log [**C3**] versus response with a variable slope and four parameters.

#### 2.17. *T. cruzi*-infected mice treatments

Animals were infected (as described above) and treated 8 h after infection, up to the ninth dpi, twice a day (12/12 h). Mice received the compounds (**C1** or **C3**) at a dose of 1 mg/Kg by gavage (orally) or intraperitoneal routes. The control group received a vehicle solution. The parasitemia level was determined as described above. In the second experiment, infected mice were treated 8 h after infection, up to the ninth dpi with **C3** loaded into the NE system or with Bz, both at doses of 10 mg/kg by gavage (orally), once a day. The control group received an empty NE solution. Parasitemia level and survival were monitored.

### 3. Results

#### 3.1. Characterization of the 4-chlorophenylthioacetone-derived thiosemicarbazones and hydrazones

Microanalyses and high-resolution mass spectra were compatible with formation of **C1**-**C4**. In the infrared spectra of **C1** and **C3**, absorptions at 1520–1591 cm<sup>-1</sup> were attributed to  $\nu$ (C=N). The vibrations attributed to  $\nu$ (C=S) were observed at 848 cm<sup>-1</sup> and 864 cm<sup>-1</sup> (compounds **C1** and **C3**, respectively). For the hydrazones, the vibrations attributed to  $\nu$ (C=O) were observed at 1650 cm<sup>-1</sup> and 1685 cm<sup>-1</sup> (compounds **C2** and **C4**, respectively).

NMR spectra were recorded in DMSO-*d*<sub>6</sub>. The <sup>1</sup>H resonances were assigned on the basis of chemical shifts, multiplicities and by using 2D homonuclear <sup>1</sup>H-<sup>1</sup>H correlation spectroscopy (COSY). The carbon type (C, CH) was determined by using distortionless enhancement by polarization transfer (DEPT-135) experiments and the assignments were made by 2D heteronuclear multiple quantum coherence (HMQC) and heteronuclear multiple bond coherence (HMBC) experiments.

Formation of **C1-C4** was evidenced in the  $^1\text{H}$  NMR spectra by the presence of a signal corresponding to N2H in the 9.12–10.55 ppm range. In the  $^{13}\text{C}$  NMR spectra a signal close to 150 ppm was assigned to the iminic carbon.

Duplicated signals were observed in the  $^1\text{H}$  NMR spectra (see Supplementary Material), which corresponded to a mixture of *E* (89–96%) and *Z* stereoisomers (11–4%) in solution, as confirmed by Two-dimensional Nuclear Overhauser Effect Spectroscopy (NOESY) spectra which showed intramolecular  $^1\text{H}$ – $^1\text{H}$  coupling involving C8CH<sub>3</sub> and N2H. In the  $^{13}\text{C}$  NMR spectra, the signals did not appear to be duplicates because of the low concentration of the *Z* isomer in solution.

X-ray crystallography analyses showed that the thiosemicarbazones **C1** and **C3** crystallized in the monoclinic and triclinic systems, respectively. The compounds crystallized in the *EE* conformation in relation to the C8-N1 and C10-N2 bonds. The bond lengths (Å) and angles of the thiosemicarbazones were similar. The C10-S2 and C8-N1 bond distances were close to 1.685 and 1.272 Å, respectively, as expected for C=S and C=N double bonds [31]. Crystal data and refinement results are listed in Table S1 (Supplementary Material). The atom arrangements and atom numbering scheme for **C1** and **C3** are shown in Fig. 2. Selected intramolecular bond distances and angles are in Table S2 (Supplementary Material).

### 3.2. C1 and C3, but not C2 and C4, induce trypanocidal activity without presenting host cell toxicity

The anti-*T. cruzi* activities of **C1–C4** was evaluated in MO cultures. Dose-response data were obtained for **C1**. Infected cells treated with doses of 30, 40, or 50  $\mu\text{M}$ , presented a reduced number of amastigotes 48 h after infection and treatment, when compared with unstimulated infected cells (Fig. 3A). At a dose of 20  $\mu\text{M}$ , **C1** failed to induce anti-*T. cruzi* activity (Fig. 3A). Infected-MOs in the presence of DMSO (0.5% v/v), the maximum percentage used in our assays, and maximum concentration allowed for cell cultures [32], had similar amounts of amastigotes at 48 h compared to unstimulated infected-cells, which shows that this low DMSO content did not influence the results (Fig. 3A).

As no significant difference was observed among the numbers of intracellular parasites found in stimulated macrophages incubated with 30, 40, or 50  $\mu\text{M}$  of **C1** (Fig. 3A), the lowest concentration was chosen for subsequent experiments. The other compounds (**C2**, **C3**, and **C4**), which are structurally similar to **C1**, were tested in infected-MO cultures, and only **C3** was able to reduce amastigote replication when compared to unstimulated infected cells (Fig. 3B). In the assay to test decreasing doses of **C3**, it was observed that at all tested concentrations, **C3** efficiently controlled intracellular *T. cruzi* replication at 48 h (Fig. 3C). At 20  $\mu\text{M}$ , **C3** showed higher anti-*T. cruzi* activity than at 10  $\mu\text{M}$ , and since activity of **C3** was similar at 20  $\mu\text{M}$  and 30  $\mu\text{M}$ , the 20  $\mu\text{M}$  condition was chosen for the subsequent experiments. Additionally, the LDH-

cytotoxicity assay demonstrated that even at the highest concentration used (50  $\mu\text{M}$ ), the thiosemicarbazones **C1** or **C3** did not induce toxicity to the host cells (Fig. 3D). Similar to the results found with infected-MOs stimulated with the compounds, only **C1** and **C3** had direct activity against the epimastigote form of the parasite (Fig. 3E).

### 3.3. C1 and C3 attenuate T. Cruzi growth in macrophage cultures independently of nitric oxide production

After initial screening, we started a more detailed analysis of the trypanocidal activity of **C1** and **C3** compared to stimulation with the IFN- $\gamma$  cytokine (a potent inducer of MO trypanocidal activity). As shown in Fig. 4A, infected cells stimulated with **C1** presented a lower parasitic load compared to unstimulated infected cells at both 24 and 48 h after treatment, and this effect was similar to the IFN- $\gamma$  activity. Regarding parasite uptake, the presence of **C1** did not alter the capacity of trypanomastigote invasion in MOs (Fig. 4B). Moreover, **C1** treatment also reduced the release of trypanomastigotes when compared to unstimulated infected cells (Fig. 4C). Of note, treatment with **C3** presented the highest capacity to control amastigote replication, even higher than IFN- $\gamma$  (Fig. 4D), and decreased parasite uptake/invasion (Fig. 4E) and trypanomastigotes release by infected-MOs (Fig. 4F).

Next, the involvement of NO, IL-6, and TNF cytokines in the anti-*T. cruzi* activity induced by **C1** or **C3** in infected cells was investigated. Moreover, to exclude the requirement of NO in macrophage activity by compounds, iNOS deficient macrophages (iNOS KO) were used. Fig. 4G and 4I demonstrated that at the time of analysis, only IFN- $\gamma$  stimulus was able to induce NO production by infected MOs. In fact, NO production triggered by iNOS was not necessary for the trypanocidal activity of the compounds under study here, because WT or iNOS KO MOs showed similar trypanocidal capacity when treated with **C1** (Fig. 4H) or **C3** (Fig. 4J). **C1** or **C3** induced the uninfected MOs to secrete TNF (Fig. 4K), but not IL-6 (Fig. 4K). When these cells were infected, treatment with **C3**, but not with **C1**, increased TNF production, compared with the unstimulated infected group. On the other hand, treatment with **C1**, but not with **C3**, decreased IL-6 levels when compared to the unstimulated infected group (Fig. 4K). Moreover, ROS production, the enzyme IDO, and NO were not necessary for maintaining the microbicidal activities induced by **C1** or **C3** in *T. cruzi*-infected MOs. Phox KO MOs, in the presence or absence of LNMMA (NO production inhibitor), and IDO KO macrophages reduced the parasite number in macrophages when stimulated with **C1** or **C3** (Fig. S18, Supplementary Material).

### 3.4. C3 controls trypanomastigote release by cardiomyocytes without inducing nitric oxide, TNF, and IL-6 production

The microbicidal activity of **C3** was also evaluated in non-phagocytic H9c2 cardiomyocytes cells. Infected cardiomyocytes stimulated with

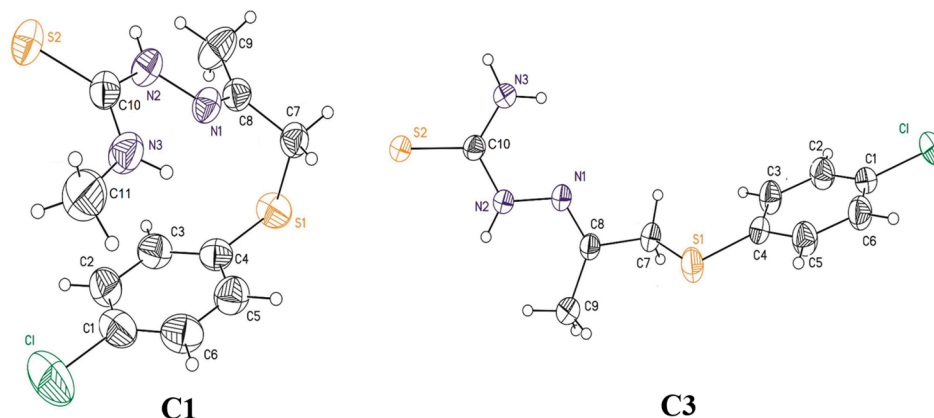
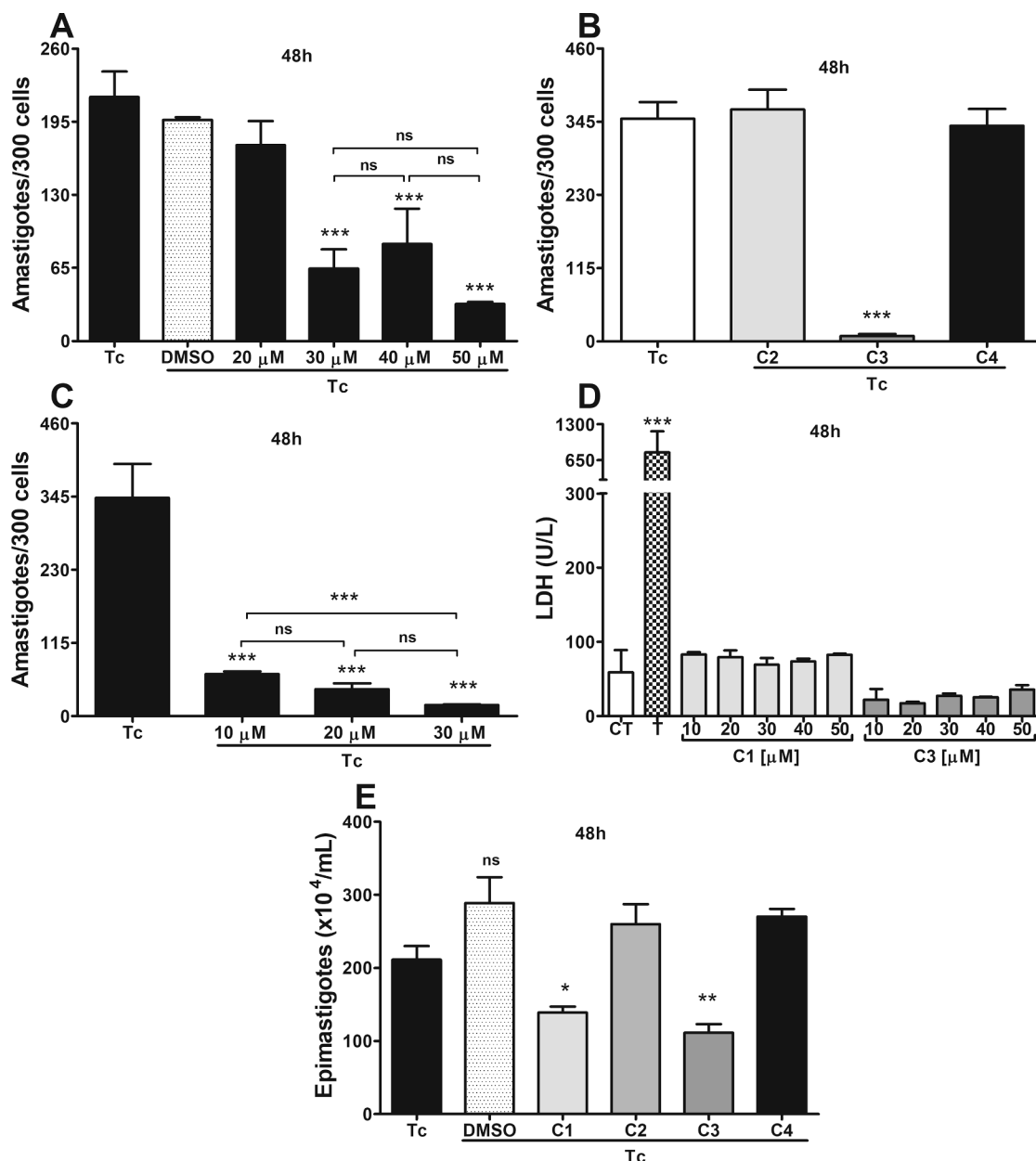


Fig. 2. Molecular plots of **C1** and **C3** showing the labeling scheme of the non-H atoms and their displacement ellipsoids at the 50% probability level.



**Fig. 3.** C1 and C3, but not C2 and C4, attenuate *T. cruzi* replication in macrophages and on epimastigote axenic cultures. MOs from mice (C57BL/6) were cultured, infected (5:1 - *T. cruzi*:cell ratio), and stimulated, or not, with C1 (50 to 20 μM) or in the presence of 0.5% DMSO (A) or stimulated by C2 (30 μM), C3 (30 to 10 μM), or C4 (30 μM) (B). Next, intracellular parasite counts were performed on fixed and stained cells at 48 h (C). MOs were cultured in the presence of C1 (30 μM), C3 (20 μM), or culture medium only, and after 48 h, the supernatants were collected for toxicity assessment (LDH). For the positive lysis control, 2% triton was used (D). Epimastigotes (Y strain) were incubated, or not, in the presence of C1–C4 (30 μM) or DMSO 0.5%, and 48 h after incubation, parasite replication analysis was performed (E). Each point represents the mean ± SEM of one of the two independent experiments, \* =  $p \leq 0.05$ ; \*\* =  $p < 0.01$ ; \*\*\* =  $p < 0.001$ . (ns = not significant).

C3, in all tested concentrations, reduced trypomastigote release when compared to unstimulated infected cells (Fig. 5A). The dose of 2.5 μM was chosen for the next tests, because it sufficiently controlled parasite release and was not toxic to the host cell (Fig. 5B). Treatment with C3 and IFN-γ did not induce NO (Fig. 5C), TNF (Fig. 5D), or IL-6 (Fig. 5E) production by cardiomyocytes at 48 h after treatment.

### 3.5. C1 and C3 act directly on trypomastigote forms of the parasite and in different stages of macrophage infection to decrease parasite release

First, to determine whether the compounds could pre-activate the host cell microbicidal response against *T. cruzi* before infection, MOs were pre-treated with C1 or C3 for 1 h, and the cells were washed before

infection. As shown in Fig. 6A, when MOs pre-treated with C1 or C3 were infected, there was a lower parasite release at the seventh dpi, without uptake impairment (Fig. 6B). In order to investigate the possible direct activity of compounds on *T. cruzi*, trypomastigotes were incubated with or without C1 or C3 for 1 h before infection. MOs that were infected with parasites pre incubated with C1 or C3 showed decreased number of released trypomastigotes from the fourth to seventh dpi, when compared with parasites pre-incubated with medium alone (Fig. 6C). Moreover, pre-incubation with C1 or C3 reduced capacity of parasites to invade the host cells (Fig. 6D). Next, we investigated whether C1 or C3 could act at different stages of *T. cruzi* infection, mainly by directly inhibiting proliferation and differentiation of amastigotes in trypomastigotes. C1 reduced the number of trypomastigotes released when added

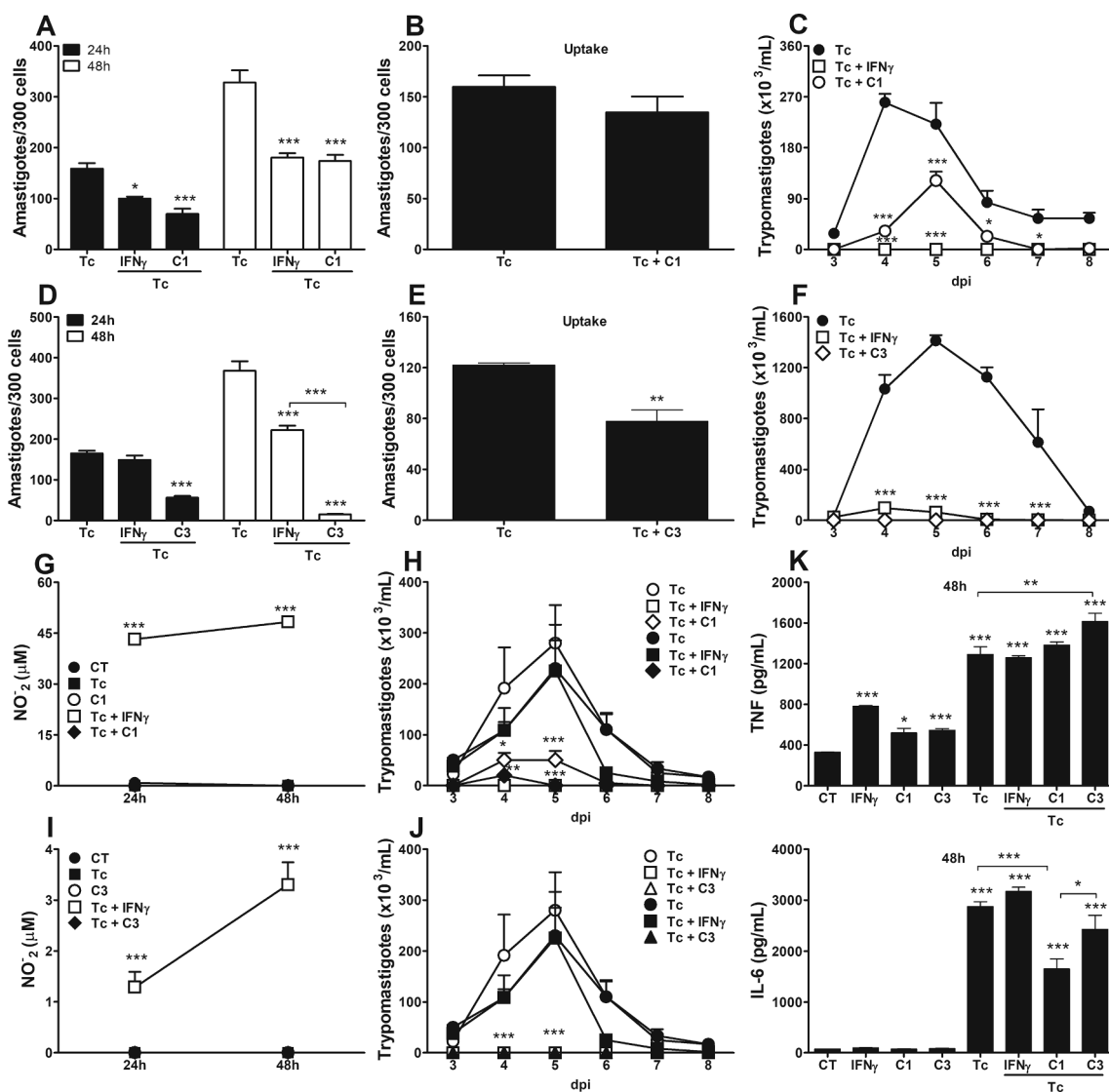


**Fig. 4.** C1 and C3 control amastigote replication and trypomastigote release in macrophages, independent of NO production. WT or iNOS KO peritoneal MOs were plated and/or infected with trypomastigote forms and stimulated, or not, with compounds. Intracellular amastigote count was performed at 24 h and 48 h after infection and treatment with C1 (30  $\mu$ M) (A) or C3 (20  $\mu$ M) (D). For a positive control of *T. cruzi* intracellular replication, IFN- $\gamma$  100 ng/mL was used. Parasite uptake was evaluated 4 h after simultaneous infection and treatment with C1 (30  $\mu$ M) (B) or C3 (20  $\mu$ M) (E). Trypomastigote release was followed from the third to seventh dpi after C1 treatment (30  $\mu$ M) (C), or with C3 (20  $\mu$ M) (F), and after C1 (30  $\mu$ M) treatment in WT (empty symbols)  $\times$  iNOS KO (filled symbols) MOs (H) or C3 (20  $\mu$ M) treatment in WT (empty symbols)  $\times$  iNOS KO (filled symbols) MOs (J). At 24 h and 48 h intervals, supernatants were collected for NO dosing (G–C1 treatment; I–C3 treatment) and cytokine measurements after treatment with C1 or C3 (K): TNF – top panel; IL-6 – bottom panel. “CT” (control) = uninfected and unstimulated cells. Each point represents the mean  $\pm$  SEM of one of two independent experiments, \* =  $p \leq 0.05$ ; \*\* =  $p < 0.01$ ; \*\*\* =  $p < 0.001$ .

to the culture at different times after infection (a.i.): 4 h (Fig. 6E), 12 h (Fig. 6F), 24 h (Fig. 6G), and 48 h (Fig. 6H). C1 also reduced the number of parasites when added to cultures at 4, 12, and 24 h a.i. Of note, C3 displayed a potent trypanocidal capacity, as did IFN- $\gamma$ , and drastically reduced the number of amastigotes in cells and trypomastigotes in the culture supernatant when added to culture after all analyzed infection times (Fig. 6E–H). These results strongly suggest that compounds C1 and C3 have direct activity on *T. cruzi*.

To confirm the direct action of compounds on the parasite, free trypomastigotes were pre-incubated with C1, C3 or benznidazole (Bz, used as positive control) for 1 h, or incubated with the compounds for all times analyzed. As shown in Fig. 6I, a decreased parasite number was observed 12 and 24 h after the initial treatment for 1 h with C1 or C3, respectively. In the assay where the parasites remained in contact with the compounds during all analysis times, after 2 h of incubation, C1 decreased the number of parasites (Fig. 6J). After 6 h of incubation, both

C1 and C3 reduced the number of parasites, when compared to the control (parasite incubated with medium alone) and, of great relevance, to the group incubated with Bz. At 12 h of incubation, C1 and C3 continued to decrease the number of parasites; and only at this time after incubation was it possible to observe the trypanocidal activity of Bz, which took place 10 h later than that of C1 and 6 h after that of C3 (Fig. 6J). Through the MTT assay, we observed that the incubation of epimastigotes with C1 or C3, but not with Bz, decreased parasite viability within 4 h of treatment (Fig. 6K).

### 3.6. C1 and C3 decrease the number of circulating parasites in the blood of mice

The potential therapeutic capacities of C1 and C3 were investigated in an acute model of *T. cruzi* infection. Our results showed that the treatment of infected animals with C1 reduced the number of parasites

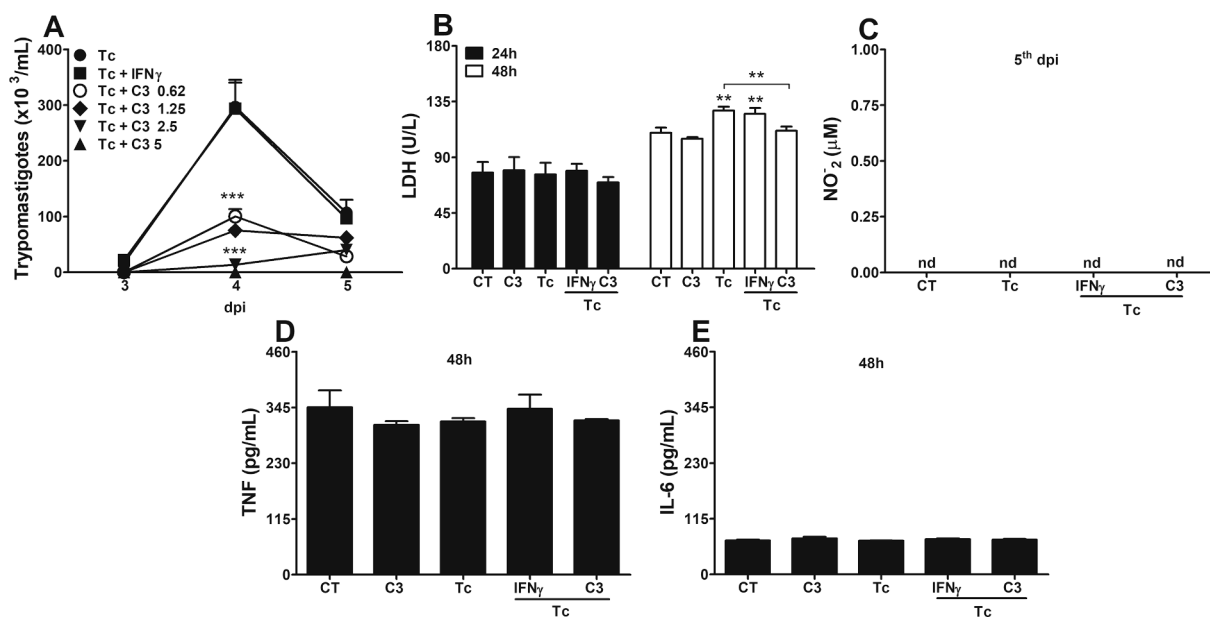


**Fig. 5.** C3 protects H9c2 cardiomyocytes from *T. cruzi* lytic activity, independently of cytokine (TNF and IL-6) and NO production. H9c2 CMs were cultured, infected (5:1 - *T. cruzi*:cell ratio), and stimulated, or not, with C3 (5 to 0.6  $\mu$ M). Subsequently, trypomastigotes release was followed from the third to fifth dpi (A). Infected-CMs were cultured in the presence of C3 (2.5  $\mu$ M), IFN- $\gamma$  (100 ng/mL), or culture medium only. After 24 and 48 h, the supernatants were collected for toxicity assessment (LDH) (B). At the fifth dpi, the supernatants were collected for NO measurement (C). The supernatants were also collected at 48 h to evaluate cytokine production; TNF (D) and IL-6 (E). Each point represents the mean  $\pm$  SEM of one of two independent experiments, \* =  $p \leq 0.05$ ; \*\* =  $p < 0.01$ ; \*\*\* =  $p < 0.001$ .

in the blood of animals at both the seventh and ninth dpi when administered orally and at the seventh dpi when administered intraperitoneally (Fig. 7A). C3 reduced the level of parasitemia at both the seventh and ninth dpi by both routes of administration (Fig. 7B).

### 3.7. *T. cruzi*-topoisomerase-3 $\alpha$ is involved in parasite resistance to C1, but not to Bz and C3

First, we evaluated whether the activities of C1 and C3 were trypanocidal or trypanostatic against epimastigote forms. As seen in the growth curves of the parasites (Fig. 8A), the presence of C1 and C3 inhibited parasite growth.

To check whether the growth inhibition was due to immediate DNA damage caused by C1 and C3 that led to the activation of the DNA damage response, we analyzed the effect of caffeine on the activities of C1 and C3. For this, epimastigotes were pre-incubated with caffeine, which is an ATM/ATR (kinases that function as the main damage sensor during DNA Damage Response; DDR) pathway inhibitor. To choose an inhibitor concentration, the parasites were incubated with increasing doses of caffeine, and the growth curve was monitored. We found that the concentrations of 1, 2, or 4 mM of caffeine did not change the parasite growth pattern at all times observed, when compared to the control group (Fig. S19, Supplementary Material), with an intermediate dose of 2 mM. Next, epimastigotes were incubated with caffeine at 2 mM for 1 h, then "washed" to remove the compound, and immediately afterwards, seeded in culture plates and incubated with Bz, C1, or C3. Inhibition of the ATM/ATR pathway by caffeine did not change the capacity of C1 or C3 to control parasite growth (Fig. 8B).

In another approach, we investigated whether the absence of *T. cruzi* topoisomerase-3 $\alpha$  could alter the control pattern of parasitic replication exhibited in the presence of C1 and C3, since this enzyme plays an important role during DNA duplication and repair. In Fig. 8C we can see that Topo-3 $\alpha$  knockout parasites were more susceptible to C1 anti-*T. cruzi* activity. Notably, both WT and KO parasites were highly susceptible to the anti-*T. cruzi* action induced by C3 (Fig. 8C). The ability of C1 and C3 to inhibit the cruzain enzyme was also evaluated. For this,

experiments were carried out in which cruzain was incubated in the presence of the compounds at 100  $\mu$ M and later, the fluorescent substrate was added, and its cleavage was measured by fluorescence emission. Initially, C3 was able to inhibit cruzain, with  $IC_{50} = 41 \pm 5 \mu$ M (Fig. 8D). An additional assay was carried out to verify whether the observed enzyme inhibition by C3 was due to nonspecific inhibition. It is known that small molecules can aggregate and inhibit enzyme activity in a non-specific manner. A feature of inhibitory aggregates is that non-ionic detergents can disrupt their formation and reduce their influence on enzyme inhibition [33,34]. In detergent tests, a 31% change in C3 activity was observed when comparing 0.1% with 0.001% Triton X-100. Taken together, the sensitivity of C3 to detergent, its low potency against cruzain, and the absence of cruzain inhibition by the structurally related C1 indicates that the trypanocidal activity of C3 is not due to cruzain inhibition.

### 3.8. C3 loaded in lipid NE maintains anti-*Trypanosoma cruzi* activity in vitro and in vivo

In order to improve its pharmacological properties, C3 was subjected to encapsulation in nanoemulsion (NE). The characterization results showed particles with an average diameter close to 180 nm and a narrow size distribution ( $PI < 0.30$ ), indicating a monodisperse system. The zeta potential was slightly negative, probably due to the free fatty acids present on the NE surface. The EE (%) was close to 100%, which demonstrates that practically all of the added compound was properly encapsulated inside the nanostructures (Fig. 9A).

Our biological results demonstrated that encapsulated C3 maintained anti-*T. cruzi* activity, similar to that of C3 in its free form, as demonstrated by the reduction of trypomastigote release by MOs, from the third to fifth dpi (Fig. 9B), without inducing toxicity to the host cells (Fig. 9C). In an animal model of acute chagasic infection, our results showed that infected animals treated with the formulation containing C3 reduced the parasitemia at the peak of infection (Fig. 9D). The same phenotype was observed with Bz treatment (Fig. 9D). Of note, treatment with the C3 formulation, but not with Bz, increased the survival

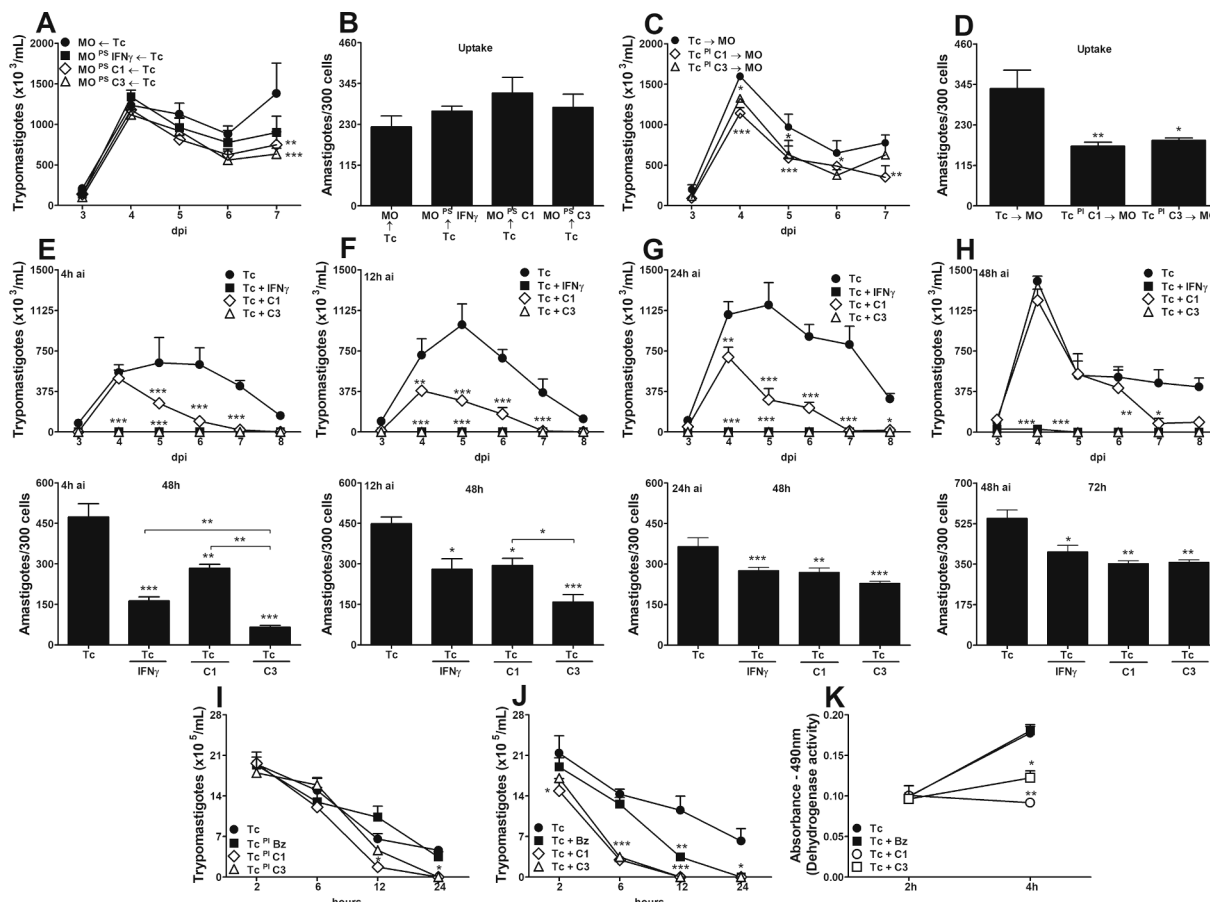


**Fig. 6.** C1 and C3 act directly on trypomastigotes, faster than benznidazole, and infected-cells by reducing replicative capacity and amastigote differentiation. Peritoneal MOs were plated and stimulated, or not, with C1 (30  $\mu$ M), C3 (20  $\mu$ M), or IFN- $\gamma$  100 ng/mL for a period of 1 h. After this interval, cells were washed with RPMI medium and infected, and trypomastigotes release was followed from the third to seventh dpi (A). Cells were in simultaneous contact (parasite + compounds [C1 or C3 or IFN- $\gamma$ ], or parasite only) for a period of 4 h, to evaluate the parasite entry profile (uptake) in the host cells (B). Trypomastigotes were incubated, or not, in the presence of C1 (30  $\mu$ M) or C3 (20  $\mu$ M) for a period of 1 h. After this time, parasites were centrifuged to remove the compounds, and plated MOs were posteriorly infected with pre-incubated trypomastigotes, and trypomastigote release was followed from the third to seventh dpi (C). Additionally, parasites went through the same process described before and were in contact with MOs for 4 h (pre-incubated trypomastigote uptake) (D). MOs were plated and infected with trypomastigotes, and after 4 h (E), 6 h (F), 12 h (G) or 24 h (H) post infection, compounds were added, and trypomastigote release (panel above) and amastigote replication/differentiation (panel below) were analyzed. Trypomastigotes were cultured in the presence of RPMI alone, C1 (30  $\mu$ M), C3 (20  $\mu$ M), or benznidazole (30  $\mu$ M) for 1 h. After this time, the parasites were centrifuged to remove the compounds and plated (96 wells-plate) (I), or the trypomastigotes remained throughout the analysis in the presence of the compounds (J). Quantitation of the viable parasites was performed at 2, 6, 12 and 24 h after previous treatment (optical microscope) and at 2 and 4 h after incubation, by the MTT assay (K). Each point represents the mean  $\pm$  SEM of one of the two independent experiments, \* =  $p \leq 0.05$ ; \*\* =  $p < 0.01$ ; \*\*\* =  $p < 0.001$ .

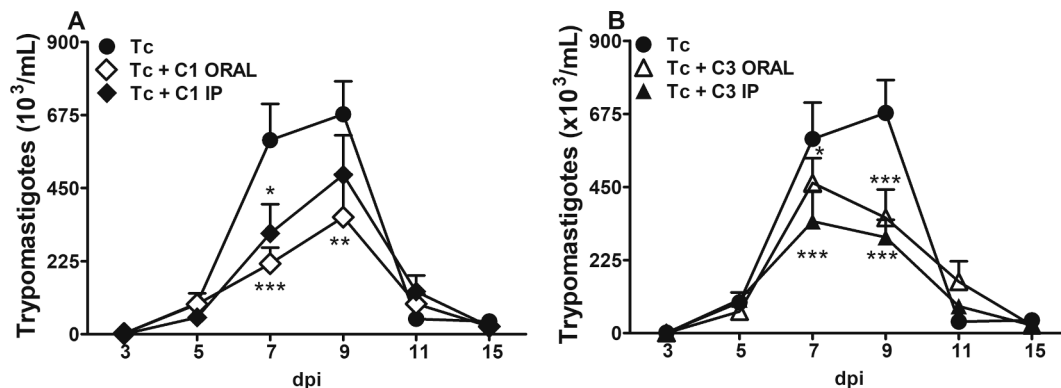


**Fig. 7.** C1 and C3 decrease parasitemia in *T. cruzi*-infected mice. Female C57BL/6 mice were infected (1x10<sup>3</sup> trypomastigotes - Y strain) and treated with C1 (A) or C3 (B) at 1 mg/Kg by gavage (ORAL) or intraperitoneal (IP) routes for 12/12 h. From the third to fifteenth dpi, blood was collected through the caudal vein every two days for parasite quantification. "Tc" = infected animals. "Tc + C1" = infected animals treated with C1. "Tc + C3" = infected animals treated with C3. \* =  $p \leq 0.05$ ; \*\* =  $p < 0.01$ ; \*\*\* =  $p < 0.001$  in relation to the infected group treated with the infection control. Each point represents the mean  $\pm$  SEM of one of the two independent experiments.

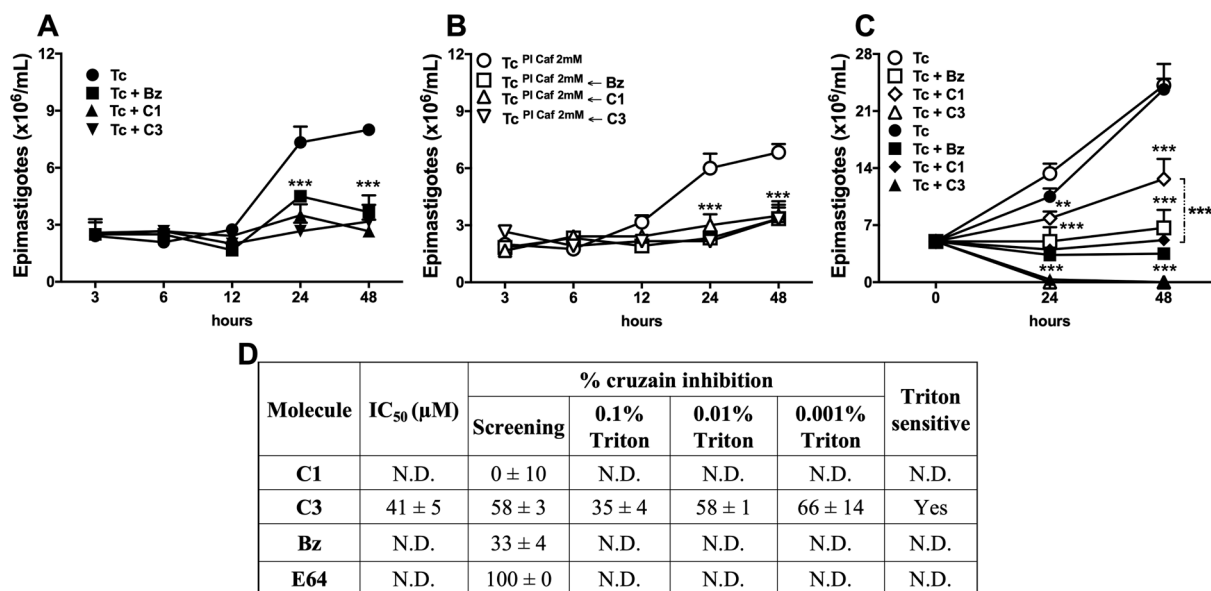


**Fig. 8.** Evaluation of the involvement of the ATM/ATR pathway, the Topo-3 $\alpha$  enzyme, and cruzain inhibition in the anti-*T. cruzi* activity of C1 or C3. Epimastigotes (Y strain) were pre-treated, or not (A), with caffeine (2 mM) for 1 h (B), and subsequently incubated, or not, in the presence of the compounds (A, B). Parasite growth was followed at 3, 6, 12, 24, and 48 h after treatment with C1, C3, or Bz molecules (A, B). \*\*\* =  $p < 0.001$  (in comparison to the treated group with the untreated control). WT (DM28 strain; empty symbols) or Topo-3 $\alpha$  KO (filled symbols) epimastigotes were cultured and treated, or not, with 30  $\mu$ M C1, C3, or Bz. Parasite growth was evaluated at 24 and 48 h after treatment (C). \*\* =  $p < 0.01$ ; \*\*\* =  $p < 0.001$  (in comparison to the treated group with the untreated control). Each point represents the mean  $\pm$  SEM of one of the two independent experiments. To determine the compound IC<sub>50</sub>, cruzain (4 nM) was incubated in the presence of 100  $\mu$ M C1, C3, or Bz for 10 min. Then, 2.5  $\mu$ M of the substrate, Z-Phe-Arg-aminomethylcoumarine (Z-FR-AMC), was added to start the reaction. To assess the sensitivity to detergent inhibition (triton X-100), the compounds [IC<sub>50</sub> - 0.01% triton X-100] were pre-incubated with a solution containing cruzain and 0.001%, 0.01%, or 0.1% triton X-100 for 10 min. Then, a substrate solution with the same concentration of triton X-100 was added to the plates, and the fluorescence was monitored. Reported values refer to the average and standard deviation obtained from two independent experiments, in triplicate. "N.D." = not determined (D).

percentage during the time investigated (Fig. 9E).

#### 4. Discussion

Chemotherapies with benznidazole and nifurtimox have been used as the gold standard for treating ChD for more than half a century. However, Bz and Nfx therapies require long-term treatment that is associated with potential side effects, and the effectiveness of using these drugs for complete parasite elimination remains unclear. In this context, we investigated the trypanocidal activity of new thiosemicarbazones (C1 and C3) and hydrazones (C2 and C4) derived from 4-chlorophenylthioacetone.

Our results showed that among the studied compounds, only C1 and C3 controlled the intracellular replication of *T. cruzi* in MOs. In fact, C2 and C4 were not able to control *T. cruzi* proliferation in MOs. The same phenomenon was observed in the axenic culture of epimastigotes, where C1 and C3 limited the replication of the parasites, while C2 and C4 did not show any anti-*T. cruzi* activity. Hence, we may infer that replacement of the sulfur atom by oxygen completely abolishes the anti-trypanosomal activity of the 4-chlorophenylthioacetone-derived Schiff bases.

The presence of extracellular LDH (in the culture supernatant) is a fundamental characteristic of cells undergoing apoptosis, necrosis, and other forms of cell damage [27]. Our results showed that even at higher doses, C1 and C3 did not induce toxicity (increased extracellular LDH) in the host cells.

In the context of ChD, the IFN- $\gamma$  production or administration correlates with resistance to *T. cruzi* infection, mainly in the acute phase [35]. Our data showed that C1 has similar trypanocidal activity to IFN- $\gamma$ , while C3 has a higher activity than IFN- $\gamma$  *in vitro*. Our experiments were designed to mimic a scenario where parasites complete their intracellular cycle and are released into the bloodstream, at a point at which patients would receive treatment with C1 or C3 (where MOs were

exposed simultaneously to the compounds and the parasite). The results revealed that in the presence of C3, but not C1, parasite invasion into the uninfected cells was decreased. These results are extremely important and indicate that C3 interferes with the parasite-cell interaction to reduce parasite proliferation and dissemination of the infection.

Studies with humans and experimental animal models suggest the involvement of the immune system in the effectiveness of many drug treatments [36], including the dependence of "immunological factors" for Bz therapeutic activity [37]. Thus, we investigated whether immunological mechanisms were involved in the microbicidal activity of C1 or C3 in macrophages. In this context, the investigation of NO production is relevant, since this compound can act directly on the parasite to induce its death [38]. However, our results showed that the trypanocidal activities of C1 and C3 in infected MOs were independent of NO production and/or the presence of the iNOS enzyme.

TNF and IL-6 cytokines are also important mediators of *T. cruzi* infection and exert protective effects against the parasite [39,40]. Thiosemicarbazone C3 increased TNF production and maintained IL-6 secretion levels by infected-MOs, which may contribute to the greater microbicidal activity of C3 in relation to C1.

ROS production has been reported as a mechanism of resistance against various infections [41]. In the context of *T. cruzi* infection, low ROS concentrations promote signaling for parasite proliferation. However, in high "doses," ROS behaves as toxic agents against the parasite [42].

Our results showed that the inhibition of NADPH oxidase activity by the absence of the catalytic subunit gp<sup>91phox</sup> did not cause any interruption of the anti-*T. cruzi* activity triggered by C1 or C3 in the MOs. Other pathways, such as those that induce nutrient deprivation, are also important for limiting intracellular pathogen growth [43]. Hence, we investigated whether the activity of the IDO enzyme (resistance can correlate with Trp deprivation and/or the generation of metabolites produced by IDO activity that are toxic to the parasite) could be involved

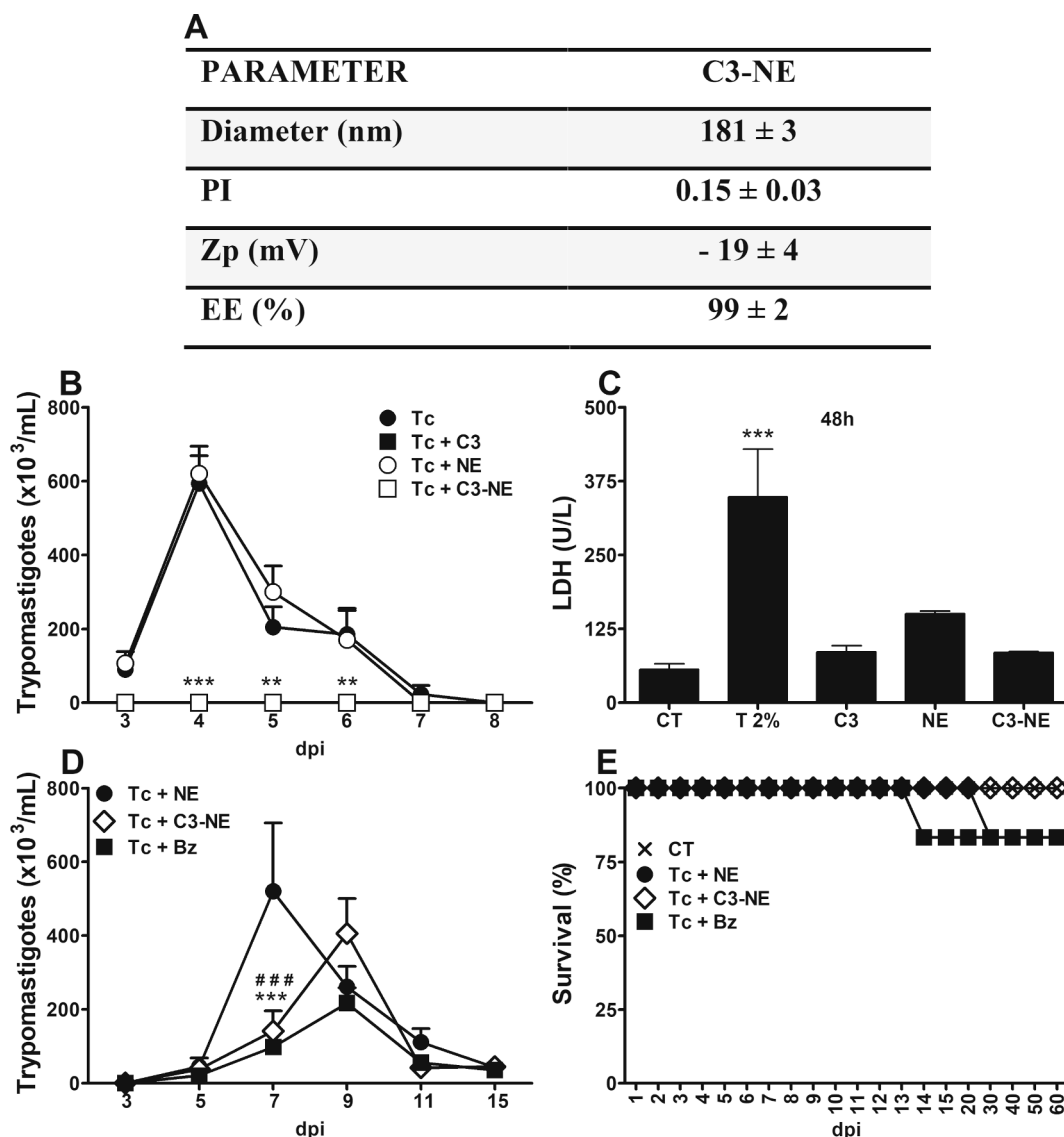


**Fig. 9.** The effect of NE containing C3 on *T. cruzi* infection *in vitro* and *in vivo*. Parameters including particle diameter, polydispersity index (PI), Zeta potential (Zp), and encapsulation efficiency (EE) were evaluated after the construction of the nanosystem (A). MOs from mice (C57BL/6 – female) were cultured, infected (5:1 - *T. cruzi*:cell ratio), and stimulated, or not, with free or encapsulated C3 at 20  $\mu$ M. Trypomastigote release was followed from the third to eighth dpi after C1 treatment (B). After 48 h, the supernatants were collected for toxicity assessment (LDH). For the positive lysis control, 2% triton (T) was used (C). C57BL/6 mice were infected ( $1 \times 10^3$  trypomastigotes – Y strain) and treated, or not, with C3-NE (nanoemulsion) or Bz (Benznidazole) at 10 mg/Kg by oral route, once a day. From the third to fifteenth dpi, blood was collected every two days for parasite (D) and survival (E) evaluations. “CT” = non-infected cells/animals. “Tc” = infected cells/animals. “Tc + C3” = infected cells treated with C3 (free). “Tc + NE” = infected cell/animals treated with empty NE. “Tc + C3-NE” = infected cells/animals treated with NE containing C3. “Tc + Bz” = infected animals treated with Benznidazole. \*\*\* =  $p < 0.001$  (Tc + NE  $\times$  Tc + Bz), # # # =  $p < 0.001$  (Tc + NE  $\times$  Tc + C3-NE). Each point represents the mean  $\pm$  SEM of one of the two independent experiments.

in the trypanocidal mechanism of C1 or C3 in MOs. Our data demonstrated that IDO deficiency did not cause a loss in the trypanocidal activity triggered by C1 or C3 in MOs, which indicates that this pathway does not participate in the microbicidal activity of these molecules.

The investigation of the anti-*T. cruzi* activity of C3 in cardiomyocytes (a cell type of extreme importance due to its involvement in the cardiac pathophysiology of ChD) revealed that, unlike IFN- $\gamma$ , the treatment of infected cardiomyocytes with C3 decreased the release of trypomastigotes, independent of NO, TNF, and IL-6 production. Furthermore, the treatment of infected-CMs with C3 protected against the lithic activity of *T. cruzi* (maintenance of LDH levels similar to that of uninfected cells).

Collectively, the results obtained with MOs and CMs strongly suggest that the thiosemicarbazones C1 and C3 act mainly by mechanisms that induce direct death of the parasite, independently of the activation of the main “classical” host cell microbicidal mechanisms described so far

(i.e., NO and ROS production).

To understand the role of host cells in the trypanocidal mechanisms of C1 and C3, host cells were pre-incubated with C1 or C3 before infection. The compounds were still able to control the release of trypomastigotes by MOs without changing the parasite invasion capacity in pre-stimulated cells.

Here, the direct activity of C1 and C3 on parasites was demonstrated. Pre-incubation of the trypomastigotes with the compounds led to a reduced number of parasites released in the supernatant correlated with the reduced invasion capacity of pre-incubated parasites. This indicates that the compounds may act either indirectly or directly on the parasites to control their replication in MOs.

Our data obtained through the treatment of MOs, beginning after different times of infection, suggest that C1 and C3 effectively inhibited amastigote replication and differentiation. Of great relevance, our

results from the direct incubation of trypomastigotes with **C1** and **C3** strongly suggest that these compounds act to directly induce the parasite death, faster than Bz, without the need for the host cell microbicidal machinery. Validating our findings *in vitro*, we found that, importantly, **C1** or **C3** maintained their anti-*T. cruzi* activity in an animal model of acute chagasic infection, decreasing the parasitemia level of the infected animals. However, further studies *in vivo* are required to compare the efficacy of the treatments with **C1**, **C3** and BZ, and to demonstrate the molecular mechanisms responsible for the observed effects.

Based on the results of the compounds' direct activity on the parasites, we investigated certain signaling pathways and molecular targets on which the compounds could act to lead to parasite death. First, we investigated whether **C1** and **C3** induce the parasite death through a signaled response, more precisely, via ATM/ATR signal transducer kinases. Our results suggest that the ATM/ATR pathway does not play a role in the maintenance of anti-*T. cruzi* activity exerted by **C1**, **C3**, or Bz, since pre-incubation of parasites with an inhibitor of this pathway, caffeine (cells treated with caffeine exhibit various phenotypic abnormalities reported in cells with ATM or ATR function deficiency) [44], did not impair the anti-*T. cruzi* action of the compounds. This suggests that the action of **C1** and **C3** was not immediate, but that it causes delayed damage that blocks parasite duplication without immediate DNA damage response (DDR) activation.

Contrary to the results obtained with the inhibition of ATM/ATR enzymes, the absence of topoisomerase-3 $\alpha$  in the parasite resulted in a greater trypanocidal capacity of **C1**, which demonstrates that the presence of this enzyme is important for parasite resistance against the action of **C1**. This compound probably induces damage to the DNA of the parasite, in which topoisomerase and other enzymes are involved in its repair.

Our findings demonstrated that among all the tested compounds, only **C3** inhibited the catalytic activity of cruzain, with an IC<sub>50</sub> = 41.5  $\mu$ M. However, further assays indicated that this moderate inhibition is likely due to nonspecific mechanisms. Together, our results showed that the mechanisms involving Topo-3 $\alpha$  activity were more involved in the trypanocidal activity of the compounds than in the cellular mechanisms that require the participation of the ATM/ATR pathway and cruzain activity.

The low solubility of several thiosemicarbazones in an aqueous medium [45], may impair absorption and therefore, their therapeutic effects. Many researchers have resorted to the use of organic solvents, such as DMSO, for solubilizing these compounds. However, DMSO can induce adverse effects at levels that are not yet well defined in humans [46]. Therefore, we incorporated **C3** into a lipid nanosystem for drug delivery (NE), to improve its absorption and therapeutic action. Our results showed that the nanosystem that contained **C3** was able to control *T. cruzi* infection *in vitro* and *in vivo*, and thus, has potential to provide a safer strategy for the treatment of ChD.

## 5. Conclusions

In summary, our data demonstrate the potential therapeutic effects of the 4-chlorophenylthioacetone-derived thiosemicarbazones **C1** and **C3** against *T. cruzi* infection in both isolated parasites and host infected cells, with reduction of parasite proliferation and dissemination. Of note, **C1** and **C3** were effective against all evolutionary forms of the parasite (epimastigotes, trypomastigotes, and amastigotes), acting faster than BZ. Treatment with **C3** loaded in a lipid nanocarrier system was more efficient than treatment with BZ, preventing death during experimental infection. The obtained results constitute an important contribution to the development of new pharmacological strategies for the treatment of ChD.

### Funding

This work was supported by Conselho Nacional de Desenvolvimento Científico e Tecnológico (CNPq: 305894/2018–8), Coordenação de Aperfeiçoamento de Pessoal de Nível Superior (CAPES-Brazil), National

Institute for Science and Technology in Dengue and Host-microbial interactions (Programa INCT; APQ-03606–17), INCT-INOVAR (CNPq 465.249/2014–0) and Fundação de Amparo à Pesquisa do Estado de Minas Gerais, Rede Mineira de Imunobiológicos (FAPEMIG; REDE-00140–16) and FAPEMIG APQ-00628–16.

## Declaration of Competing Interest

The authors declare that they have no known competing financial interests or personal relationships that could have appeared to influence the work reported in this paper.

## Acknowledgements

The authors would like to thank Dr. M. A. Ribeiro, Departamento de Química (Universidade Federal do Espírito Santo, Brazil) and Jacqueline Barbosa de Oliveira Viana (Universidade Federal de Minas Gerais, Brazil) for technical assistance. We also thank Allison Doak and Dr. Brian Shoichet, from the University of California San Francisco, for gently providing recombinant cruzain.

## Appendix A. Supplementary data

Supplementary data to this article can be found online at <https://doi.org/10.1016/j.bioorg.2021.105018>.

## References

- [1] World health organization: Chagas disease (American trypanosomiasis). (2020).
- [2] J.R. Coura, *Tripanosomose, doença de Chagas, Cienc. Cult.* 5 (2003) 1.
- [3] F.R. Gutierrez, Regulation of Innate Immunity During Trypanosoma cruzi Infection, in: Control Innate Adapt. Immune Responses Dur. Infect. Dis., Springer, 2011: pp. 69–84. [https://doi.org/10.1007/978-1-4614-0484-2\\_4](https://doi.org/10.1007/978-1-4614-0484-2_4).
- [4] M.N. Alvarez, L. Piacenza, F. Irigoín, G. Peluffo, R. Radi, Macrophage-derived peroxynitrite diffusion and toxicity to Trypanosoma cruzi, Arch. Biochem. Biophys. (2004), <https://doi.org/10.1016/j.abb.2004.09.015>.
- [5] G. Peluffo, L. Piacenza, F. Irigoín, M.N. Alvarez, R. Radi, L-arginine metabolism during interaction of Trypanosoma cruzi with host cells, Trends Parasitol. (2004), <https://doi.org/10.1016/j.pt.2004.05.010>.
- [6] C.P. Knubel, F.F. Martínez, R.E. Fretes, C. Díaz Lujan, M.G. Theumer, L. Cervi, C. C. Motrán, Indoleamine 2,3-dioxygenase (IDO) is critical for host resistance against Trypanosoma cruzi, FASEB J. (2010), <https://doi.org/10.1096/fj.09-150920>.
- [7] F.S. Machado, G.A. Martins, J.C.S. Aliberti, F.L.A.C. Mestriner, F.Q. Cunha, J. S. Silva, Trypanosoma cruzi-infected cardiomyocytes produce chemokines and cytokines that trigger potent nitric oxide-dependent trypanocidal activity, Circulation. (2000), <https://doi.org/10.1161/01.CIR.102.24.3003>.
- [8] J.R. Coura, S.L. De Castro, A critical review on Chagas Disease chemotherapy, Mem. Inst. Oswaldo Cruz. (2002), <https://doi.org/10.1590/S0074-02762002000100001>.
- [9] G.M.S. Da Silva, M.F.F. Mediano, P.E.A.A. Do Brasil, M. Da Costa Chambela, D.J. A. Silva, A.S. De Sousa, S.S. Xavier, A.R. Da Costa, R.M. Saraiva, A.M. Hasselcher-Moreno, A clinical adverse drug reaction prediction model for patients with Chagas Disease treated with benznidazole, Antimicrob. Agents Chemother. (2014), <https://doi.org/10.1128/AAC.02842-14>.
- [10] A.P.A. Oliveira, A.A. Recio-Despaigne, I.P. Ferreira, R. Diniz, K.A.F. Sousa, T. M. Bastos, M.B. Pereira Soares, D.R.M. Moreira, H. Beraldo, Investigation of the antitrypanosomal effects of 2-formyl-8-hydroxyquinoline-derived hydrazones and their antimony(III) and bismuth(III) complexes, New J. Chem. (2019), <https://doi.org/10.1039/c9nj02676b>.
- [11] C. Rodrigues, A.A. Batista, J. Ellena, E.E. Castellano, D. Benítez, H. Cerecetto, M. González, L.R. Teixeira, H. Beraldo, Coordination of nitro-thiosemicarbazones to ruthenium(II) as a strategy for anti-trypanosomal activity improvement, Eur. J. Med. Chem. (2010), <https://doi.org/10.1016/j.ejmech.2010.03.005>.
- [12] A. Pérez-Rebolledo, L.R. Teixeira, A.A. Batista, A.S. Mangrich, G. Aguirre, H. Cerecetto, M. González, P. Hernández, A.M. Ferreira, N.L. Speziali, H. Beraldo, 4-Nitroacetophenone-derived thiosemicarbazones and their copper(II) complexes with significant in vitro anti-trypanosomal activity, Eur. J. Med. Chem. (2008), <https://doi.org/10.1016/j.ejmech.2007.06.020>.
- [13] M.Z. Hernandez, M.M. Rabello, A.C.L. Leite, M.V.O. Cardoso, D.R.M. Moreira, D. J. Brondani, C.A. Simone, L.C. Reis, M.A. Souza, V.R.A. Pereira, R.S. Ferreira, J. H. McKerrow, Studies toward the structural optimization of novel thiazolylhydrazones-based potent antitrypanosomal agents, Bioorganic Med. Chem. (2010), <https://doi.org/10.1016/j.bmc.2010.09.056>.
- [14] L.B. Costa, M.V. De Oliveira Cardoso, G.B. De Oliveira Filho, P.A.T. De Moraes Gomes, J.W.P. Espíndola, T.G. De Jesus Silva, P.H.M. Torres, F.P. Silva, J. Martín, R.C.B.Q. De Figueiredo, A.C.L. Leite, Compound profiling and 3D-QSAR studies of

- hydrazone derivatives with activity against intracellular *Trypanosoma cruzi*, *Bioorganic, Med. Chem.* (2016), <https://doi.org/10.1016/j.bmc.2016.02.027>.
- [15] M. Sajid, S.A. Robertson, L.S. Brinen, J.H. McKerrow, Cruzain: The path from target validation to the clinic, *Adv. Exp. Med. Biol.* (2011), [https://doi.org/10.1007/978-1-4419-8414-2\\_7](https://doi.org/10.1007/978-1-4419-8414-2_7).
- [16] R.B. Da Silva, C.R. Machado, A.R. Aquiles Rodrigues, A.L. Pedrosa, Selective human inhibitors of ATR and ATM render leishmania major promastigotes sensitive to oxidative damage, *PLoS One.* (2018), <https://doi.org/10.1371/journal.pone.0205033>.
- [17] M. Gonzales-Perdomo, S.L. De Castro, M.N.S.L. Meirelles, S. Goldenberg, *Trypanosoma cruzi* proliferation and differentiation are blocked by topoisomerase II inhibitors, *Antimicrob. Agents Chemother.* (1990), <https://doi.org/10.1128/AAC.34.9.1707>.
- [18] T. Cunha Almeida, L.H. Gonzaga Ribeiro, L.B. Ferreira dos Santos, C.M. da Silva, R. Tupinambá Branquinho, M. de Lana, F. Ramos Gadelha, A. de Fátima, Synthesis, in vitro and in vivo anti-*Trypanosoma cruzi* and toxicological activities of nitroaromatic Schiff bases, *Biomed. Pharmacother.* (2018), <https://doi.org/10.1016/j.biopha.2018.09.176>.
- [19] K. Čerpnjak, A. Zvonar, M. Gašperlin, F. Vrečer, Lipid-based systems as a promising approach for enhancing the bioavailability of poorly water-soluble drugs, *Acta Pharm.* (2013), <https://doi.org/10.2478/acph-2013-0040>.
- [20] Oxford Diffraction, CrysAlisPro CCD and CrysAlisPro RED, Oxford Diffraction Ltd, Yarnton, Oxfordshire, England, 2010.
- [21] G.M. Sheldrick, Crystal structure refinement with SHELXL, *Acta Cryst.* (2015), <https://doi.org/10.1107/S2053229614024218>.
- [22] G.M. Sheldrick, SHELXL-2014/7: Program for the Solution of Crystal Structures (2014).
- [23] A.L. Spek, Structure validation in chemical crystallography, *Acta Crystallogr. Sect. D Biol. Crystallogr.* (2009), <https://doi.org/10.1107/S090744490804362X>.
- [24] D.L. Klayman, J.F. Bartosevich, T.S. Griffin, C.J. Mason, J.P. Scovill, 2-Acetylpyridine Thiosemicarbazones. 1. A New Class of Potential Antimalarial Agents, *J. Med. Chem.* (1979), <https://doi.org/10.1021/jm00193a020>.
- [25] A. Barroso, M. Gualdrón-López, L. Esper, F. Brant, R.R.S. Araújo, M.B.H. Carneiro, T. V. ávila, D.G. Souza, L.Q. Vieira, M.A. Rachid, H.B. Tanowitz, M.M. Teixeira, F.S. Machado, The aryl hydrocarbon receptor modulates production of cytokines and reactive oxygen species and development of myocarditis during *Trypanosoma cruzi* infection, *Infect. Immun.* (2016), <https://doi.org/10.1128/IAI.00575-16>.
- [26] L.C. Green, D.A. Wagner, J. Glogowski, P.L. Skipper, J.S. Wishnok, S. R. Tannenbaum, Analysis of nitrate, nitrite, and [15N]nitrate in biological fluids, *Anal. Biochem.* (1982), [https://doi.org/10.1016/0003-2697\(82\)90118-X](https://doi.org/10.1016/0003-2697(82)90118-X).
- [27] P. Kumar, A. Nagarajan, P.D. Uchil, Analysis of cell viability by the lactate dehydrogenase assay, *Cold Spring Harb. Protoc.* (2018), <https://doi.org/10.1101/pdb.prot095497>.
- [28] W.D. DaRocha, R.A. Silva, D.C. Bartholomeu, S.F. Pires, J.M. Freitas, A.M. Macedo, M.P. Vazquez, M.J. Levin, S.M.R. Teixeira, Expression of exogenous genes in *Trypanosoma cruzi*: Improving vectors and electroporation protocols, *Parasitol. Res.* (2004), <https://doi.org/10.1007/s00436-003-1004-5>.
- [29] N.C. Fonseca, L.F. Da Cruz, F. Da Silva Villela, G.A. Do Nascimento Pereira, J.L. De Siqueira-Neto, D. Kellar, B.M. Suzuki, D. Ray, T.B. De Souza, R.J. Alves, P.A.S. Júnior, A.J. Romanha, S.M.F. Murta, J.H. McKerrow, C.R. Caffrey, R.B. De Oliveira, R.S. Ferreira, Synthesis of a sugar-based thiosemicarbazone series and structure-activity relationship versus the parasite cysteine proteases rhodesain, cruzain, and *Schistosoma mansoni* cathepsin B1, *Antimicrob. Agents Chemother.* (2015), <https://doi.org/10.1128/AAC.04601-14>.
- [30] G.A.N. Pereira, E.B. da Silva, S.F.P. Braga, P.G. Leite, L.C. Martins, R.P. Vieira, W. T. Soh, F.S. Villela, F.M.R. Costa, D. Ray, S.F. de Andrade, H. Brandstetter, R. B. Oliveira, C.R. Caffrey, F.S. Machado, R.S. Ferreira, Discovery and characterization of trypanocidal cysteine protease inhibitors from the 'malaria box', *Eur. J. Med. Chem.* (2019) <https://doi.org/10.1016/j.ejmech.2019.06.062>.
- [31] F.H. Allen, O. Kennard, D.G. Watson, L. Brammer, A.G. Orpen, R. Taylor, Tables of bond lengths determined by x-ray and neutron diffraction. Part 1. Bond lengths in organic compounds, *J. Chem. Soc. Perkin Trans. 2* (1987), <https://doi.org/10.1039/P29870000051>.
- [32] LifeTein® LLC, Peptide Synthesis: Handling and Storage of Synthetic Peptides, (2017). [https://www.lifetein.com/handling\\_and\\_storage\\_of\\_synthetic\\_peptides.html](https://www.lifetein.com/handling_and_storage_of_synthetic_peptides.html).
- [33] R.S. Ferreira, C. Bryant, K.K.H. Ang, J.H. McKerrow, B.K. Shoichet, A.R. Renslo, Divergent modes of enzyme inhibition in a homologous structure-activity series, *J. Med. Chem.* (2009), <https://doi.org/10.1021/jm9009229>.
- [34] B.K. Shoichet, Screening in a spirit haunted world, *Drug Discov. Today.* (2006), <https://doi.org/10.1016/j.drudis.2006.05.014>.
- [35] R. McCabe, S. Meagher, B. Mullins, Gamma interferon suppresses acute and chronic *Trypanosoma cruzi* infection in cyclosporin-treated mice, *Infect. Immun.* (1991).
- [36] B.J. Berger, A.H. Fairlamb, Interactions between immunity and chemotherapy in the treatment of the trypanosomiasis and leishmaniasis, *Parasitology.* (1992). <https://doi.org/10.1017/S0031182000075375>.
- [37] A.J. Romanha, R.O. Alves, S.M.F. Murta, J.S. Silva, C. Ropert, R.T. Gazzinelli, Experimental Chemotherapy against *Trypanosoma cruzi* Infection: Essential Role of Endogenous Interferon- $\gamma$  in Mediating Parasitologic Cure, *J. Infect. Dis.* (2002). <https://doi.org/10.1086/342415>.
- [38] G.N.R. Vespa, F.Q. Cunha, J.S. Silva, Nitric oxide is involved in control of *Trypanosoma cruzi*-induced parasitemia and directly kills the parasite in vitro, *Infect. Immun.* (1994), <https://doi.org/10.1128/IAI.62.11.5177-5182.1994>.
- [39] J.S. Silva, G.N.R. Vespa, M.A.G. Cardoso, J.C.S. Aliberti, F.Q. Cunha, Tumor necrosis factor alpha mediates resistance to *Trypanosoma cruzi* infection in mice by inducing nitric oxide production in infected gamma interferon-activated macrophages, *Infect. Immun.* (1995). <https://doi.org/10.1128/IAI.63.12.4862-4867.1995>.
- [40] W. Gao, M.A. Pereira, Interleukin-6 is required for parasite specific response and host resistance to *Trypanosoma cruzi*, *Int. J. Parasitol.* (2002), [https://doi.org/10.1016/S0020-7519\(01\)00322-8](https://doi.org/10.1016/S0020-7519(01)00322-8).
- [41] C.N. Paiva, M.T. Bozza, Are reactive oxygen species always detrimental to pathogens?, *Antioxidants Redox Signal.* (2014). <https://doi.org/10.1089/ars.2013.5447>.
- [42] G.R. Goes, P.S. Rocha, A.R.S. Diniz, P.H.N. Aguiar, C.R. Machado, L.Q. Vieira, *Trypanosoma cruzi* Needs a Signal Provided by Reactive Oxygen Species to Infect Macrophages, *PLoS Negl. Trop. Dis.* (2016), <https://doi.org/10.1371/journal.pntd.0004555>.
- [43] R. Appelberg, Macrophage nutritive antimicrobial mechanisms, *J. Leukoc. Biol.* (2006). <https://doi.org/10.1189/jlb.0206079>.
- [44] J.N. Sarkaria, E.C. Busby, R.S. Tibbetts, P. Roos, Y. Taya, L.M. Karnitz, R.T. Abraham, Inhibition of ATM and ATR kinase activities by the radiosensitizing agent, caffeine, *Cancer Res.* (1999).
- [45] K.C. Agrawal, A.C. Sartorelli, The Chemistry and Biological Activity of  $\alpha$ -(N)-Heterocyclic Carboxaldehyde Thiosemicarbazones, *Prog. Med. Chem.* (1978). [https://doi.org/10.1016/S0079-6468\(08\)70259-5](https://doi.org/10.1016/S0079-6468(08)70259-5).
- [46] B.K. Madsen, M. Hilscher, D. Zetner, J. Rosenberg, Adverse reactions of dimethyl sulfoxide in humans: A systematic review, *F1000Research.* (2019). <https://doi.org/10.12688/f1000research.16642.2>.